1 **Earth, Wind, Fire, and Pollution: A Review on Aerosol Nutrient Sources**

2 **and Impacts on Ocean Biogeochemistry**

3 Douglas S. Hamilton[1]* (0000-0002-8171-5723), Morgane M. G. Perron[2] (0000-0001-5424-7138),

4 Tami C. Bond[3] (0000-0001-5968-8928), Andrew R. Bowie[2] (0000-0002-5144-7799), Rebecca R.

5 Buchholz[4] (orcid.org/0000-0001-8124-2455), Cecile Guieu[5] (0000-0001-6373-8326), Akinori Ito[6]

6 (0000-0002-4937-2927), Willy Maenhaut[7] (0000-0002-4715-4627), Stelios Myriokefalitakis[8] (0000-

7 0002-1541-7680), Nazlı Olgun[9], Sagar D. Rathod[10] (0000-0001-7170-4302), Kerstin

8 Schepanski[11] (0000-0002-1027-6786), Alessandro Tagliabue[12] (0000-0002-3572-3634), Robert

9 Wagner[11] (0000-0001-7365-8020), and Natalie M. Mahowald[1] (0000-0002-2873-997X).

10 1: Department of Earth and Atmospheric Science, Cornell University, Ithaca, NY, USA

11 2: Institute for Marine and Antarctic Studies, University of Tasmania, Battery Point,

12 Tasmania, Australia

13 3: Department of Mechanical Engineering, Colorado State University, Fort Collins, CO,

14 USA

15 4: Atmospheric Chemistry Observations & Modeling Laboratory, National Center for

16 Atmospheric Research, Boulder, Colorado USA.

17 5: Sorbonne Université, CNRS, Laboratoire d'Océanographie de Villefranche, LOV,

18 Villefranche-sur-mer, France

19 6: Graduate School of Environmental Studies, Nagoya University, Nagoya, Japan

20 7: Department of Chemistry, Ghent University, Gent, Belgium

21 8: Institute for Environmental Research and Sustainable Development, National

22 Observatory of Athens, Penteli, Greece

23 9: Climate and Marine Sciences Division, Eurasia Institute of Earth Sciences, Istanbul

24 Technical University, 34469, Maslak, Istanbul, Turkey

25 10: Department of Atmospheric Science, Colorado State University, Fort Collins, CO,

26 USA

27 11: Leibniz Institute for Tropospheric Research, Leipzig, Germany

28 12: School of Environmental Sciences, University of Liverpool, Liverpool, UK

29 **Corresponding Author**: dsh224@cornell.edu

30 **Running Title:** Review of Nutrient Aerosol Sources

31 **Key Words:** Mineral Dust, Fires, Volcanoes, Phosphate, Soluble Iron, Ocean

32 Biogeochemistry

33 A key Earth System science question is the role of atmospheric deposition in supplying

34 vital nutrients to the phytoplankton that form the base of marine food webs. Industrial and

35 vehicular pollution, wildfires, volcanoes, biogenic debris, and desert dust all carry

36 nutrients within their plumes throughout the globe. In remote ocean ecosystems aerosol

37 deposition represents an essential new source of nutrients for primary production. The

38 large spatiotemporal variability in aerosols from myriad sources combined with the

39 differential responses of marine biota to changing fluxes makes understanding of where,

40 when, and how much nutrients from the atmosphere enter marine ecosystems of crucial

41 importance. This review brings together existing literature, experimental evidence of

42 impacts, and new atmospheric nutrient observations compared to atmospheric and ocean

43 biogeochemistry modeling. We evaluate the contribution and spatiotemporal variability of

44 nutrient-bearing aerosols from desert dust, wildfire, volcanic, and anthropogenic sources,

45 including the organic component, deposition fluxes, and oceanic impacts.

Introduction

By travelling long distances with the atmospheric flow, aerosols deliver essential nutrients to remote marine ecosystems (Baker and Jickells, 2017; Doney et al., 2009; Duce et al., 1991; Jickells et al., 2005; Kanakidou et al., 2012; Mahowald et al., 2018; Zender et al., 2004). Aerosol transport pathways and distance travelled is determined by a particle's properties (size, composition, and density), atmospheric conditions (particle uplift, buoyancy, and the wind speed and direction), and travel altitude. The smaller the particle size and the higher the altitude of travel, the greater chance for long atmospheric residence times and for reaching remote marine ecosystems (Baker and Croot, 2010). The loss of aerosol (gases) from the atmosphere proceeds by two routes: dry (direct) deposition of the aerosol (gaseous species) and wet deposition within precipitation (Baker et al., 2007). At ~362 million km^2 the world's oceans cover ~71% of the Earth's surface, providing a major sink pathway for nutrients and pollutants emitted from land. The atmospheric lifetime of aerosols ranges from a few days to weeks (Textor et al., 2006), much less than the mixing-time within-and-between hemispheres. Such short atmospheric lifetimes combined with the heterogeneous physicochemical nature of aerosol composition creates large spatial and temporal variations in observed aerosol nutrient concentration patterns between ocean regions (Figure 1). As understanding of biogeochemical cycles grows, a strong requirement arises for improved knowledge regarding how nutrients from different sources are supplied to marine ecosystems.

Conceptually, aerosol nutrient sources can be split into three groups: the first is natural in origin and includes mineral dust, wildfires, volcanoes, and biological particles (Barkley et al., 2019; Guieu et al., 2005; Jickells et al., 2005; Mahowald et al., 2008; Olgun et al.,

69   2011); the second stems from increasing anthropogenic activity (Ito, 2015; Ito et al., 2019;

70   Jickells et al., 2017; Krishnamurthy et al., 2009; Luo et al., 2008; Rathod et al., 2020); the

71   third is the atmospheric transformation of insoluble minerals, of either natural or

72   anthropogenic origin, into soluble (bioavailable) nutrients during transport by: (1) acids,

73   (2) organic ligands, and (3) photo-reductive processes (Ito, 2015; Johnson and

74   Meskhidze, 2013; Longo et al., 2016; Shi et al., 2015; Stockdale et al., 2016). In addition

75   to directly providing a new nutrient source, anthropogenic activity modifies the generation

76   of predominately natural aerosols (Ginoux et al., 2012; Hamilton et al., 2018; Mahowald

77   et al., 2010; Ward et al., 2014), and provides a source of those compounds which work

78   to liberate a fraction of minerals into more bioavailable nutrient forms (Li et al., 2017;

79   Meskhidze et al., 2005; Solmon et al., 2009). This coupling of historical human activity

80   with biogeochemical cycles is highly complex and contains many uncertainties, partly due

81   to the absence of early historical measurements and on the reliance on proxy records to

82   describe the historical evolution of natural aerosol fluxes with intensifying human activity.

83   Marine biota are a key component in the biogeochemical cycles that determine the

84   ocean's capacity to sequester atmospheric CO_2 and support marine ecosystem services

85   over different timescales. Furthermore, they emit biological gases to the atmosphere

86   which subsequently oxidize to form organic and sulphate aerosol, therefore creating

87   climate feedbacks through altering cloud properties, temperatures, and precipitation

88   rates. By relieving nutrient limitation, large aerosol deposition events have the potential

89   to modify the natural assemblage due to new resource competition among primary

90   producers. The resulting change in phytoplankton balance between smaller and larger

91   sizes (Giovagnetti et al., 2013; Paytan et al., 2009) and between autotrophic and

92   heterotrophic communities (Gazeau et al., 2020; Marañón et al., 2010) determines the

93   capacity of the ocean to sequester anthropogenic CO_2 following deposition (Guieu et al.,

94   2014a). The degree to which autotrophs or heterotrophs are stimulated depends on (1)

95   the physicochemical form in which nutrients are delivered to seawater and (2) the initial

96   biogeochemical conditions of the water column, including the physical features around

97   the depth and strength of stratification that determines the initial in situ nutrient limitation,

98   linked to the supply of macro- or micronutrients from below the thermocline (Guieu et al.,

99   2014b). Understanding the fertilization potential of aerosol is of particular interest in

100   surface waters of the Southern Ocean, where phytoplankton net primary productivity

101   (NPP) is limited by iron supply and biological response to aerosol deposition can regulate

102   the global carbon cycle (Martin, 1990; Parekh et al., 2004; Tagliabue et al., 2014) and the

103   redistribution of macronutrients to low latitudes (Sarmiento et al., 2004; Tagliabue et al.,

104   2009).

105   There has been a recent effort to review the most up-to-date knowledge on the magnitude

106   of atmospheric deposition fluxes of the main nutrient species to the oceans: Altieri et al.

107   (2021) reviewed reactive nitrogen; Jickells et al. (2017) updated anthropogenic nitrogen

108   estimates; Mahowald et al. (2018) reviewed the role of metals as nutrients and pollutants;

109   Myriokefalitakis et al. (2018) undertook a multi-model comparison for soluble iron; and

110   Kanakidou (2018) reviewed nitrogen, phosphorus, and iron chemistry and fluxes. From

111   an oceanic perspective, Boyd and Ellwood (2010) and Tagliabue et al. (2017) reviewed

112   the marine iron cycle, focusing on the impact of mineral dust deposition. Here, we build

113   upon this body of literature by reviewing current understanding and uncertainties in major

114   aerosol nutrient sources (mainly: desert dust, fires, volcanoes, biogenic particles, and

115   anthropogenic activity) and their respective spatiotemporal deposition signatures. While

116   early studies of the impact of atmospheric iron and phosphorus deposition on ocean

117   biogeochemistry often solely focused on dust, recent evidence has highlighted the

118   importance of non-dust sources (Barkley et al., 2019; Ito et al., 2019) - even suggesting

119   the carbon export efficiency (gram of atmospheric CO_2 sequestered per gram of iron

120   deposited) of non-dust iron is larger than that of dust-sourced iron (Hamilton et al., 2020a;

121   Ito et al., 2020b). To further explore the emerging role of (wild)fires in biogeochemical

122   cycles, we provide a case study of recent megafire activity in Australia during 2019-2020,

123   including recent observations and new atmospheric and ocean biogeochemical modeling

124   experiments. The characterization and individual contribution of differing aeolian

125   pathways to the ocean are important future research areas requiring better constraint to

126   improve understanding on the impact of aerosol deposition on marine biogeochemical

127   cycles historically, at present, and in the future, and to better apprehend the fast-evolving

128   human dimension.

129   **Aerosol Nutrients, Observations over Oceans, and Impacts on Biota**

130   Over the last few decades intense research efforts (e.g., SOLAS and GEOTRACES

131   research programs) have significantly advanced understanding on the oceanic impact of

132   nutrient-bearing aerosol deposition. That said, field observations are much more

133   extensive in the Northern Hemisphere due to easier logistics and cheaper cost of

134   undertaking sea-going campaigns compared to the Southern Hemisphere (Figure 1). As

135   such, the atmospheric deposition fluxes of nutrients to Southern Hemisphere oceans

136   remains highly uncertain, with soluble iron the most studied historically. The highly

137   episodic nature of aeolian dust and wildfire plumes (e.g., the range in daily iron deposition

138   maybe ≥10 orders of magnitde for some ocean regions; Hamilton et al., 2019) and an

139   increasing appreciation of the role of atmospheric processing enhancing aerosol nutrient

140   solubility during transport (Longo et al., 2016; Stockdale et al., 2016) makes data

141   acquisition of representative field observations a challenge that needs to be addressed.

142   Nitrogen is a core element for sustaining biological systems and functions, but mainly

143   found in its highly stable elemental form (dinitrogen; N_2) which is not bioavailable.

144   However, through biological nitrogen fixation by diazotrophs N_2 enters the ocean

145   biosphere and provides the largest source of bioavailable new nitrogen in the open

146   oceans (Capone et al., 1997; Jickells et al., 2017; La Roche and Breitbarth, 2005). A

147   smaller amount of reactive nitrogen (nitrogen hereafter) is available which is bioavailable

148   (Altieri et al., 2021 and references therein) and strongly associated with anthropogenic

149   sources (Jickells et al., 2017). Owing to the significant amount of literature reviewing

150   nitrogen supply, further discussion is limited.

151   Phosphorus is another vital nutrient for supporting life. Because heavy particles fall below

152   the ocean's mixed layer only phosphate may be relevant for marine biota, although

153   observations remain limited (Baker et al., 2006; Mahowald et al., 2008). Oceanic regions

154   considered co-limited by phosphate include the western North Atlantic and eastern

155   Mediterranean Sea (Moore et al., 2013). Additionally, the North Pacific Subtropical Gyre

156   can be phosphate-limited at times, oscillating with iron limitation (Letelier et al., 2019). In

157   addition to dust, wildfire and primary biogenic particles are likely to be important sources

158   of phosphate to much of the open ocean (Barkley et al., 2019; Myriokefalitakis et al.,

159   2016). Another significant fraction of phosphate, currently unaccounted for in global

160   modeling, results from the production and use of fertilizer (see below). The diversity of

161 sources partially explains why high phosphate concentrations are observed outside of

162 major dust plumes from the Northern Hemisphere dust belt and Patagonia (Figure 1).

163 Due to iron's potential to significantly modulate the marine carbon cycle (Cassar et al.,

164 2007; Martin, 1990) there has been considerable efforts placed on understanding the iron

165 cycle and its role in supporting both phytoplanktonic NPP in HNLC waters and

166 diazotrophic uptake of atmospheric N_2 at tropical latitudes. Numerous studies including

167 in-situ iron-fertilization experiments, ocean surveys, and modeling, have revealed that

168 iron-limitation of phytoplankton is the primary factor regulating NPP levels in the upwelling

169 region of the equatorial Pacific, the sub-Arctic Pacific and Atlantic oceans, and in the

170 Southern Ocean (de Baar et al., 2005; Moore et al., 2013). Here, we explore in detail the

171 role of iron supply from non-dust sources in marine biogeochemical cycles.

172 The factors that promote mineral dissolution processes, such as atmospheric acidity, the

173 presence of organic ligands, sunlight, surface-to-volume particle ratios, and ambient

174 temperature (e.g., Lasaga et al., 1994), represent one of the largest sources of

175 uncertainty in state-of-the-art model simulations. During long-range atmospheric

176 transport strong acids, such as sulfuric (H_2SO_4) and nitric (HNO_3), coat phosphorus- and

177 iron-bearing aerosol and work to liberate them into a soluble (bioavailable) form (Herbert

178 et al., 2018; Myriokefalitakis et al., 2016; Nenes et al., 2011; Shi et al., 2011). This

179 phenomena also enriches particles with nitrogen, as already observed for dust (Geng et

180 al., 2009). Such "well-mixed" deposits produce a favorable cocktail of chemical elements

181 vital for biota (N, P, Fe) being supplied to the surface ocean. The atmospheric dissolution

182 of mineral iron is also suggested to be significantly enhanced in the presence of organic

183 compounds (e.g., with oxalic acid, >75% iron solubility enhancement compared to acid

184 processing alone) (Ito, 2015; Ito and Shi, 2016; Johnson and Meskhidze, 2013;

185 Myriokefalitakis et al., 2015); see Organic Section for more discussion. Recent modeling

186 estimates that atmospheric processing creates an additional 0.56 ± 0.29 Tg soluble Fe

187 a^{-1} (Myriokefalitakis et al., 2018) and 0.030 Gg soluble P a^{-1} (Herbert et al., 2018).

188 Post-deposition processes have also been shown to affect atmospheric iron and

189 phosphorus bioavailability. It is well understood that multiple factors operate in tandem to

190 determine the fate of atmospheric dissolved iron concentrations ([dFe]), such as: iron

191 dissolution kinetics, binding ligands, scavenging, biotic uptake (Baker and Croot, 2010;

192 Boyd and Ellwood, 2010; Bressac and Guieu, 2013; Fishwick et al., 2014). Seasonal

193 variations in the ocean mixed layer affect dFe concentrations following deposition, with

194 little change during periods of deep mixed layers and the detrainment of aerosol iron

195 below the shoaling springtime mixed layer. Depending on the nature and quantity of

196 dissolved organic matter present at the time of deposition, the same dust/simulated flux

197 can provoke either iron scavenging (Wagener et al., 2010) or dissolution (Bressac and

198 Guieu, 2013; Wagener et al., 2008). Post-deposition processes for atmospheric

199 phosphorus are linked to the amount of iron-oxides present. In abiotic conditions, a

200 transient release of phosphate is usually observed in seawater, rapidly followed by a

201 strong concentration decrease due to adsorption onto iron-oxides (Louis et al., 2015,

202 2018) confirming that interactions between phosphate and iron-oxyhydroxides exert a key

203 control on phosphate availability in the environment (Chitrakar et al., 2006). Still, the role

204 of dissolved organic matter via dust-aggregation processes could in some cases, prevent

205 those interactions (Louis et al., 2015). Cellular iron quotas vary both spatially and

206 seasonally (Boyd et al., 2012, 2015; Twining et al., 2020; Twining and Baines, 2013) and

207   thus play a crucial role in linking changing aerosol iron supply to the response of

208   phytoplankton productivity; adding yet another complexity to understanding the

209   importance of atmospheric deposition. While new modeling efforts start to account for the

210   scavenging role of dust particles when estimating dFe (Ye and Völker, 2017), more work

211   is required to account for other aerosol iron phases, which may have distinct sizes,

212   dissolution kinetics, reactivity and organic phases.

213   Although complex processes are at play in determining the fate of atmospheric nutrients,

214   some biological response patterns are evidenced by aerosol-addition experiments using

215   seawater from different regions of the world. Figure 2 presents a compilation of those

216   data (n=70) reporting a relative change (maximum change shown) in autotroph biomass

217   following aerosol addition. Although such experiments are not fully representative of the

218   impact of atmospheric nutrient deposition to the ocean (Guieu et al., 2014b), it is the

219   parameter for which we have the most data available. Although the average experimental

220   outcome is in favor of an increase (~+80%) in Chl-a following artificial addition, in many

221   cases no response or negative impact are reported when (1) aerosol did not relieve

222   ongoing nutrient limitation (Guieu et al., 2010), (2) when initial metabolic balance toward

223   heterotrophs was reinforced by the deposition (Gazeau et al., 2020; Marañón et al.,

224   2010), or (3) when deposition induced a toxic effect (Paytan et al., 2009; Zhang et al.,

225   2019).

226   These disparities in biological response reveal that the bioavailability of chemical

227   elements carried by aerosols depends on a complex set of processes. Governing

228   parameters include the emission source and mixing processes that occurred during

229   transport, the type of deposition (dry or wet), and the biogeochemical state of the

230　seawater receiving aerosol deposition. Such experiments, which are mostly conducted

231　over a short period of time, show that the impact (positive or negative) of atmospheric

232　deposition on the biomass of autotrophs is, when it exists, rapid (a few days). To date,

233　these experiments have mainly been conducted in oligotrophic environments (Table S1)

234　and resulted in modest and short-term changes of total biomass. Overall, a mixed (i.e.,

235　with anthropogenic) aerosol source stimulated Chl-a ~50% more than dust aerosol alone

236　(dust: +70%, anthropogenic/mixed: +108%). Additional experiments are required to cover

237　the vast area of the ocean where this type of data remains lacking.

238　**The Complex Interplay of Dust and Fire Aerosol Sources**

239　Multi-model estimates of global dust emissions fall between 735 and 8186 Tg a^{-1} (median:

240　2467 Tg a^{-1}) with the highest simulated by a model which resolves particle size

241　distributions above 20µm and up to 63µm (Wu et al., 2020). About 90% of all dust

242　emissions are located in the Northern Hemisphere dust belt (Ginoux et al., 2012) but are

243　highly episodic, resulting in the majority (30-to-90%) of dust aerosol deposition to ocean

244　basins to occur over ~18 days (5%) of days in a year (Mahowald et al., 2009). Dust is a

245　significant source of mineral nutrients (Figure 3a/b) and how far deposition sustains NPP

246　is a question asked for many basins (Fung et al., 2000; Guieu et al., 2019; Martin et al.,

247　1991). Mineral dust phosphorus and iron tends to be relatively insoluble compared to

248　other sources however (Figure 3a) and, in the case of iron, while dust represents up to

249　95% of the global atmospheric budget (Mahowald et al., 2009) aluminosilicate and iron-

250　oxide minerals with extremely insoluble crystalline lattices dominate emissions (<1%

251　solubility, (Journet et al., 2008)). The composition of soils from which dust originates are

252　spatially heterogeneous, displaying significantly different characteristics over very small

253   distances (Journet et al., 2014). Soil mineralogy is therefore a critical factor in determining

254   dust fertilization potential.

255   Fires can also act as a source of bioavailable nutrients to the open ocean (Barkley et al.,

256   2019; Guieu et al., 2005; Ito et al., 2019; Paris et al., 2010) and are suggested to dominate

257   the temporal variability in iron deposition fluxes for many basins (Hamilton et al., 2020b).

258   Two different pathways to aerosol nutrient delivery can be associated with fires (Figure

259   4). The first is direct emission of aerosols, including the resuspension of terrigenous

260   particles previously deposited onto vegetation and entrainment of mineral dust particles

261   from surrounding soils into smoke plumes. Here, emissions are generally driven by the

262   pyro-dynamics of the fire and thus reflect the intensity of the event and the characteristics

263   of the fuel being consumed (Reid et al., 2005). The second pathway considers the

264   saltation and aeolian uplift of the largely bare burnt soil surface resulting from fires.

265   In-situ and lidar remote sensing suggests the presence of mineral dust particles in wildfire

266   smoke plumes (Kavouras et al., 2012; Nisantzi et al., 2014; Schlosser et al., 2017) and

267   increased dust emissions from post-fire burnt landscapes have been reported (Dukes et

268   al., 2018; Jeanneau et al., 2019; Wagenbrenner et al., 2017; Whicker et al., 2006).

269   However, the total fraction of dust (and hence phosphorus and iron) emissions caused by

270   fires has not yet been quantified. The average Fe/Al ratio compiled from 30-years' worth

271   of field campaigns investigating aerosol composition within, mainly tropical, biomass

272   burning regions (n=17; Tables S3 and S4 and Figure S1) is ~0.6. Fires are likely enriched

273   in iron above the global mean crustal ratio (0.44; McLennan, 2001) by approximately

274   one-third (~36%); in agreement with previous studies suggesting that the majority of iron

275   in grassland and forest fires comes from the surrounding soils, either directly or via

276   resuspended particles previously deposited on vegetation (e.g., Gaudichet et al., 1995;

277   Maenhaut et al., 1996; Paris et al., 2010). Compared to ordinary dust storms, fire-driven

278   (pyro-convective) dust emission allows for (a) increasing emissions of larger particles, (b)

279   entrainment at higher altitudes (Veira et al., 2015), and, if entrained in the free

280   troposphere or above, (c) longer atmospheric travel distances and associated processing,

281   e.g., 2020 Australian megafire smoke travelled across the Southern Ocean to South

282   America (Khaykin et al., 2020). In addition to the heat generated in fires determining the

283   strength of pyro-convective upwinds, high temperatures can alter soil properties and

284   morphology such as mineralogy, texture, porosity, particle size distribution, and water

285   capacity (Atanassova and Doerr, 2011; McNabb and Swanson, 1990; Pérez-Cabello et

286   al., 2006). The coupling of fires and dust emission processes likely constitutes a large

287   source of uncertainty for marine biogeochemical studies and a first estimate of enhanced

288   global dust aerosol emission fluxes, both during and following biomass burning events,

289   are discussed in Sidebars 1 and 2, respectively.

290   Nitrogen emissions from fires species are well characterized in the literature (e.g., Andrea

291   2019) but estimates of other nutrients are missing. Overall, fire iron and phosphorus each

292   contribute <1% of the total mass emitted in fires (Reid et al., 2005). Mahowald et al. (2005)

293   and Luo et al. (2008) used Amazonian biomass burning observations of phosphorus and

294   iron, respectively, to estimate emission ratios relative to black carbon (BC). As BC is a

295   product of combustion and a core component in atmospheric models this provided a

296   convenient methodology to estimate global phosphorus and iron emissions from fires

297   (Mahowald et al., 2008; Myriokefalitakis et al., 2016, 2018). Here, we extend this analysis

298   beyond the Amazonian region and find a mean Fe/BC ratio of 0.30-0.41 and P/BC ratio

299   of 0.016-0.12, suggesting that iron is being emitted at least double the rate of phosphorus

300   in fires (Tables S3 and S4). Particle size segregated observations are more limited but

301   suggest coarse sized emissions of phosphorus and iron are emitted at significantly higher

302   ratios (mean across studies: 0.026-0.25 and 0.74-0.80, respectively) than fine sizes

303   (mean across studies: 0.0013-0.010 and 0.019-0.032, respectively). Lower ratios were

304   derived using observational data to calculate linear regression coefficients (Figures S2

305   and S3) while higher values are the mean across reported literature values from only

306   those studies conducted near fire activity or reporting dry (biomass burning) season

307   values (Table S3). The lower P/BC ratios are similar to those reported by Mahowald et al.

308   (2005). Likewise, the lower fine Fe/BC ratio is similar to Luo et al. (2008) but the lower

309   coarse mode ratio is a little over half the value they reported of 1.4 based on less

310   observational data than used here. As dust emissions are mostly coarse sized particles,

311   while combustion emissions are generally fine sized, this suggests a major presence of

312   iron and phosphate from dust in fire plumes. Forest and/or less energetic ("smouldering")

313   fires may also release more nutrients compared to grassland and/or intense ("flaming")

314   fires (Figure S4). However, observations comparing nutrient content in aerosol from

315   flaming and smouldering fires are scarce. Additional study is necessary to understand

316   what fire characteristics determine their potential for nutrient delivery.

317   An early estimate by Guieu et al. (2005) estimated at ≤10% the global marine soluble iron

318   deposition comes from fires. Increased observations and process understanding lead to

319   an updated estimate of around 20% (18.4–22.5%; Table S2). Regionally and during the

320   burning (dry and warm) season, this contribution can be higher, e.g., Southern

321   Hemisphere soluble atmospheric iron and phosphorus deposition from fires and dust may

322 be similar (Barkley et al., 2019; Hamilton et al., 2020b). A linkage between fire emission

323 and enhanced aerosol solubility has been suggested downwind to burning regions,

324 however this mechanism remains unclear (Mahowald et al., 2018; Paris et al., 2010;

325 Perron et al., 2020). In the case of iron, studies have estimated solubility from fire sources

326 to be between 2% and 46%. The lowest solubilities (2%) were observed from southern

327 Europe and west African sources (Guieu et al., 2005; Paris et al., 2010), mid-range

328 solubilities are observed from Australian sources at 18% (Bowie et al., 2009) or

329 estimations based on wood composition range between 10% to 15% (Rathod et al.,

330 2020), and the highest (46%) come from a southeastern USA controlled burn laboratory

331 study (Oakes et al., 2012). The large range in reported fire iron solubilities has led to

332 differing representations within models. Some investigations propose that fire iron

333 solubility is 0% at emission with acidic and organic compounds co-emitted in fires

334 significantly enhancing solubility of both fire and dust iron sources during transport of the

335 smoke plume (Ito, 2015). Others have chosen to apply higher initial fractional solubility to

336 fire iron (compared to dust sources), e.g., 33% and 4% for fine and coarse particle sized

337 emissions, respectively (Hamilton et al., 2019). The postulate of fire plumes from

338 Australian sources being a nutrient source to downwind oceanic regions was recently

339 supported by field measurements of high aerosol iron solubility in concurrence with

340 intrinsic or remotely sensed indications of the presence of aerosol from fires in samples

341 collected at several places across Australia (Perron et al., 2020; Strzelec et al., 2020;

342 Winton et al., 2016). When implementing such field observations into an inverse model,

343 the minor source of iron from Australian bushfires was estimated to represent the

344 dominant source of soluble iron (up to 82% regionally) due to higher solubility compared

345 to mineral dust source (Ito et al., 2020a). We further explore the role of Australian

346 (wild)fires on Southern Ocean biogeochemical cycles in a case study below.

347 **Volcanic Aerosol Impacts on Marine Nutrient Supply**

348 Volcanic eruptions release large volumes of volcanic ash and aerosols into the

349 atmosphere, making them an important natural nutrient source to the open ocean,

350 especially on local-to-regional scales. The physicochemical properties and depositional

351 patterns of volcanic aerosols differ from mineral dust, wildfires, or anthropogenic sources

352 (Langmann, 2013). Volcanic ash is a size class of fragmented particles with diameters of

353 submicron to ≤2 mm; such a large particle size range affects settling velocities and hence

354 the nutrient flux to receiving water columns. The chemical composition, surface salt

355 coatings, and particle size distribution of volcanic ashes varies widely and so does the

356 array of nutrients (Duggen et al., 2007; Olgun et al., 2013) and trace metals (Hoffmann et

357 al., 2012; Mahowald et al., 2018) released.

358 The volcanic ash supply to marine environments are as high as 100 g m^{-2} in the vicinity

359 of the volcano then decreasing exponentially to values of 0.1- 0.3 g m^{-2} several hundreds

360 of kilometers away in open ocean regions (Olgun et al., 2013). The most important

361 volcanic ash deposition regions are the Equatorial Eastern Pacific, sourced by the Central

362 American Volcanic Arc, the Northwestern Pacific receiving the influence of the Kamchatka

363 and the Aleutian Islands and the Southwestern Pacific both supplied by the South

364 American volcanic arcs (Figure 5). Estimates based on marine sediment core data show

365 that 128 - 221 x10^{15} g of volcanic ash has been deposited during the last millennium into

366 the Pacific Ocean (covering ~70% HNLC regions). Remote volcanic hotspots, such as

367   Iceland and Hawaii, are also important nutrient sources to the North Atlantic and the North

368   Pacific (Figure 5).

369   In addition to volcanic ammonium-bearing clinopyroxene minerals, intense lightning

370   within volcanic eruption plumes and atmospheric processing are both important sources

371   of nitrogen bearing compounds on ash surfaces. The mineral composition of volcanic

372   ashes constitutes 45-75 wt% silica and 1.0-11.0 wt% iron, depending mainly on the

373   chemistry of the lava and eruption type. Iron solubility of volcanic ash varies significantly

374   with the highest measured in acidic (pH 1-5) solutions at 22% and lower measured in

375   buffered seawater at 0.001-1.8% (Duggen et al., 2010). There is no positive correlation

376   between the iron content of ashes and the amount of iron released into the seawater (57-

377   314 nmol Fe release per gram of ash; Olgun et al., 2011), and the most likely source for

378   the rapid iron release is suggested to be the soluble surface salt coatings in the form of

379   iron-bearing halides that are formed within the eruption plume (Duggen et al., 2010).

380   **Anthropocene Perturbations to Aerosol Nutrient Sources**

381   Increased industrial, transport, mining, and agricultural activity provide new nutrient

382   emission sources to the atmosphere, imposing a significant increasing trend in nutrient

383   (and toxicant) deposition to marine ecosystems (Hamilton et al., 2020b; Ito, 2015; Jickells

384   et al., 2017; Luo et al., 2008; Matsui et al., 2018; Myriokefalitakis et al., 2020). Additionally,

385   natural emissions are impacted by human activity through anthropogenic land use and

386   climate changes. For example, since the Industrial Revolution dust emissions may have

387   doubled (Mahowald et al., 2010) while fire emissions may have halved (Hamilton et al.,

388   2018). Overall, the hemispheric balance of aerosol nutrient deposition, and thus of NPP,

389   has likely shifted positively towards the Northern Hemisphere since the Industrial

390   Revolution (Hamilton et al., 2020a; Jickells et al., 2017; Myriokefalitakis et al., 2020).

391   Anthropogenic activity has introduced two new phosphorus sources: industrial

392   combustion and fertilizer production and use. Global combustion sources are estimated

393   to release ~22 Gg phosphate annually assuming 50% solubility at emission (Mahowald

394   et al., 2008; Myriokefalitakis et al., 2016). Fertilizer production-related emissions occur

395   during phosphate rock processing, drying, and storage, and can be mostly considered

396   bioavailable due to their intended end use for plant uptake in agricultural fields. This latter

397   new source is currently not included in phosphorus biogeochemistry studies, but we

398   suggest it could be considerably higher (on average 530 Gg a^{-1}; see SI Methods for

399   details) than combustion sources and double the amount of all other phosphate source

400   emissions (273 Gg a^{-1}) combined (Mahowald et al., 2008; Myriokefalitakis et al., 2016).

401   The relative source contributions of phosphate thus appear very different when

402   considering this source (Figure 3b).

403   Apportioning the fraction of aerosol nutrient burdens within the atmosphere to

404   anthropogenic sources has been tentatively quantified in several recent studies (e.g.,

405   Jickells et al., 2017; Lamb et al., 2021; Matsui et al., 2018). In particular, the use of

406   nitrogen and iron isotope fractionation differences could aid in distinguishing a human

407   versus natural source signal in situ (Altieri et al., 2021; Conway et al., 2019), although

408   additional fractionation associated with atmospheric chemistry during transport can also

409   influence measured values. While anthropogenic aerosol is, in general, pervasive

410   throughout the globe, some pristine aerosol regions may exist and are most likely to occur

411   in summertime over HNLC marine regions (Hamilton et al., 2014; Uetake et al., 2020).

412   That HNLC marine regions are co-located with those atmospheric regions least impacted

413   by human activity in the present suggests that future anthropogenic activity hotspots could

414   impact biogeochemical cycles if developed upwind of pristine regions (Hamilton et al.,

415   2020a; Myriokefalitakis et al., 2020). Future NPP is predicted to reduce owing to

416   increased ocean stratification under future warming ocean conditions (Wang et al., 2015).

417   Increased anthropogenic nutrient fluxes may (partially) offset such reductions, however,

418   if human activity preferentially increases nitrogen and phosphate deposition, marine

419   ecosystems may further shift towards iron or other micronutrient limitation (Letelier et al.,

420   2019; Mahowald et al., 2018).

421   **The Organic Nutrient Fraction**

422   Observations compiled by Kanakidou et al. (2012) suggest that ~35% of both aerosol

423   nitrogen (3-90%) and phosphorus (20-83%) could be organic in nature, while modeling

424   suggests a corresponding deposition flux fraction of around ~20-25% for nitrogen

425   (Kanakidou et al., 2016) and up to ~50% for phosphorus (Myriokefalitakis et al., 2016).

426   Recent biogeochemistry model calculations showed that when organic nutrients are

427   considered, substantial increases in nitrogen-fixation was simulated in the tropical Pacific

428   and Atlantic Oceans but it was balanced by decreases elsewhere (up to ~40%) due to

429   the additional nitrogen inputs through organics (Myriokefalitakis et al., 2020). Although

430   the overall impact of atmospheric organic nutrient inputs to the ocean on marine NPP is

431   generally estimated low on a global scale (~2.4%), stronger regional changes are

432   calculated within the oligotrophic subtropical gyres, where the additional atmospheric

433   nitrogen deposition can support extra production of up to 15-20% (Myriokefalitakis et al.,

434   2020).

435 The atmospheric organic nitrogen fraction has a strong anthropogenic component while
436 organic phosphorus is mainly found in natural phosphorus-bearing aerosols such as
437 bioaerosols (Figure 3a). Primary biogenic particles are leaf pieces, bacteria, fungi spores,
438 or pollen released into the atmosphere either deliberately by biota or accidentally through
439 entrainment by strong winds (Després et al., 2012; Jaenicke et al., 2007; Mahowald et
440 al., 2008). Although poorly studied, most authors suggest higher concentrations above
441 high productivity forests. For example, above the Amazon forest, estimates suggest 30%
442 of the <10μm particles are primary biogenic particles (Graham et al., 2003). Since most
443 life forms have elevated phosphorus (Redfield ratios suggest ~0.5%) compared to crustal
444 content (<0.1%), primary biogenic particles are thought to be an important source of
445 phosphorus to the atmosphere, although much of this phosphorus is enclosed within large
446 particles which fall close to the emission source (Brahney et al., 2015; Tipping et al.,
447 2014). Biogenic particles are likely to contain mostly bioavailable phosphorus, and thus
448 they may represent the most important source of soluble phosphorus to many ocean
449 regions (Myriokefalitakis et al., 2016).

450 On the other hand, organic-bound iron is produced during transport when iron-containing
451 aerosols undergo organic ligand-mediated dissolution processes (i.e., as Fe(II/III)-oxalate
452 complexes). Of atmospheric organic ligands, oxalic acid is currently considered the most
453 important species and is used as a proxy for organic ligand iron-dissolution processes
454 since: (1) it is thought to be the most abundant in the atmosphere and (2) it is the most
455 effective ligand in promoting iron solubilization through the formation of iron–oxalate
456 complexes at the mineral's surface which polarize and weaken Fe–O bonds (e.g., Ramos
457 et al., 2014). Oxalic acid is produced within the atmosphere by aqueous-phase

458   photochemical processes, mainly in cloud droplets (e.g., Myriokefalitakis et al., 2011).

459   Biogenic VOCs are the most important precursors and owing to a strong source, intense

460   photochemistry, and a strong convective transport potential, high oxalate (the

461   deprotonated form of oxalic acid) concentrations are found in tropical regions

462   (Myriokefalitakis et al., 2011). However, dicarboxylic acids in the atmosphere may also

463   have various primary sources including biomass burning, vehicular exhausts, and cooking

464   emissions. Dicarboxylic acids show, nevertheless, a strong correlation with elemental

465   carbon and levoglucosan (Cao et al., 2017; Cong et al., 2015) and high concentrations of

466   oxalic acid have been observed during the Amazonian burning season (Kundu et al.,

467   2010). This suggests that biomass burning (rather than coal combustion or vehicular

468   exhaust) could be an additional atmospheric source of oxalate (Schmidl et al., 2008;

469   Yamasoe et al., 2000). Some studies postulated that high temperatures generated by

470   fires may catalyze the transformation of insoluble iron oxides in soils into more labile forms

471   in the presence of organic matter (Ito et al., 2018). Such modified soils are entrained into

472   the atmosphere both during and post-fire (Sidebars 1 and 2).

473   **Australia: A Major Nutrient Source to Southern Hemisphere Oceans**

474   Australia is one of the largest arid regions in the Southern Hemisphere, along with

475   Patagonia in South America and the Kalahari and Namib deserts in southern Africa. The

476   central 'Outback' region of Australia is composed of large sandy deserts towards the west

477   and arid geological basins (lake Eye and Murray-Darling) on the east. Australian

478   atmospheric circulation is divided into three main aerial pathways, potentially irrigating:

479   (1) the Indian Ocean via the "north-west dust path"; (2) the Tasman Sea and southern

480   Pacific downwind from the "south-east dust path"; and (3) the Great Australian Bight

481 through a smaller atmospheric depression blowing south-westwards across Western

482 Australia southern coast. Large dust storms frequently emphasize the uplift and transport

483 processes of iron-bearing dust in Australia, with mega-tons of red soil particles being

484 carried away to surrounding marine areas (Gabric et al., 2010; Mackie et al., 2008).

485 Current modeling projections suggest that Australia accounts for 10% (4-30%) of dust

486 deposited into the Southern Ocean, 7% (3-11%) of dust deposited into the Indian Ocean,

487 and 68% (20-81%) of dust deposited into the South Pacific (Kok et al., 2021).

488 In addition to being a major dust source, southern Australia is frequently hit by devastating

489 summertime wildfires, e.g., the summers of 2002-03, 2005-06, 2006-07, 2009 and 2012-

490 13 and 2018-19 (Tasmania only) (Bureau of Meteorology, http://www.bom.gov.au/).

491 Recently, the 2019-20 Australian megafires had an unprecedented impact on Australia's

492 vegetation, burning no less than 21% of the country's temperate and broadleaf forests

493 (Boer et al., 2020). Fire-induced pyrocumulonimbus clouds associated with this natural

494 disaster have been followed across the whole Southern Hemisphere, evidencing major

495 and long-lasting (over months) perturbations of the atmospheric composition (including

496 the stratosphere) in the entire Southern Hemisphere. The magnitude and elevation

497 attained by the 2020 Australian fire plume was compared to atmospheric perturbation

498 following the strongest volcanic eruption of the past 30 years (Khaykin et al., 2020).

499 Recent time series (2016-2020) observations, from samples collected at Mt. Wellington

500 in Tasmania (42.9°S, 147.2°E), reveals the aeolian transport of nutrients from Australia

501 southwards and into the Southern Ocean. Total and soluble iron measurements are

502 compared with two atmospheric iron models in Figure 6a: IMPACT (Ito et al., 2021) and

503 MIMI (Hamilton et al., 2020b) (SI Methods); see SI Methods. The four-year field

504 observations show that, during burning periods, atmospheric iron loading is significantly

505 higher than during non-fire days regardless of the season. This further suggests that

506 wildfires are a non-negligible source of iron to Australian atmospheric transport pathways.

507 While biomass contains small amounts of iron, this raises the question of which

508 mechanism leads fires emission to entrain a significant number of iron-bearing particles

509 within their plumes (Figures 4 and 5, and Sidebars 1 and 2).

510 Dust alone requires extensive atmospheric processing to reach high aerosol iron solubility

511 measured in field observations - often exceeding 10% over much of the Southern

512 Hemisphere (Baker et al., 2013; Perron et al., 2020; Winton et al., 2015). Iron modeling

513 currently includes dust, anthropogenic combustion, and fire sources of iron

514 (Myriokefalitakis et al., 2018). Comparison of ensemble modeling to Mt. Wellington

515 observations suggest fidelity in representing the total mass of iron emitted from Australia

516 (Figure 6a). However, while the observed soluble iron range on fire-days (defined when

517 intrinsic measurement of levoglucosan >10 ng m^{-3}) is captured, the median (2.5 ng m^{-3})

518 is lower than that observed (4.0 ng m^{-3}). Furthermore, modeling significantly

519 underestimates median iron solubility for non-fire days (observed: 5.9%, IMPACT: 1.2%,

520 MIMI: 3.1-3.6%), suggesting (1) the existence of a currently unaccounted for, and

521 important, atmospheric source of highly soluble iron emitted on these days or (2) that

522 processing of dust iron happens at a faster rate than currently realized under pristine

523 conditions.

524 The contribution of each source to soluble iron concentrations between models is different

525 (Figure 6b); IMPACT emphasizes dust while MIMI emphasizes fires. The increased

526 contribution of fires to soluble iron concentrations on fire-days is also higher in MIMI

527   compared to IMPACT (51-79% increase versus 38%). As near future predictions warn for

528   an increasing occurrence of conditions prone to the ignition of megafires in temperate

529   regions of Australia (Dowdy et al., 2019; Di Virgilio et al., 2019), more constraint on the

530   properties of fire sourced iron, including its pyrogenic fraction, is therefore needed.

531   We quantify the impact of the 2020 Australian megafires on ocean biogeochemistry using

532   the PISCES model (Aumont et al., 2015) and compare with previous years (Figure 6c).

533   To isolate fire impacts the model was run twice (SI Methods), with and without fire iron

534   deposition, and the difference between them analyzed for January-February (Australian

535   peak fire activity). Model soluble iron from fire was predicted using daily QFED emissions

536   as this represented the maximum Australian emission estimate and also simulated

537   median soluble iron concentrations closest to observations (observations: 4.0 ng m^{-3},

538   IMPACT: 0.9 ng m^{-3}, MIMI-FINN: 2.4 ng m^{-3}, MIMI-QFED: 4.5 ng m^{-3}). Large variability in

539   fire activity between years increases Southern Ocean (30-65°S) NPP between 1.1% and

540   3.5%, with the second largest increase, by 3.0%, occurring in 2020. As fires also

541   represent a large source of nitrogen and phosphate (Figure 3a), 3% additional NPP may

542   be a conservative estimate of the potential marine stimulation following atmospheric

543   deposition of fire aerosol. In earlier modeling work, the combined addition of nitrogen and

544   iron together (such as in fire plumes) was shown globally to induce larger NPP than a

545   single element supply would (Krishnamurthy et al., 2009).

546   In these experiments fire deposition of soluble iron has a clear overall positive impact on

547   NPP in subarctic and Southern Ocean HNLC regions (Figure 7). Depending on year, fires

548   increased annual global NPP up to 0.7% (Southern Ocean: 0.7-1.3%, central Pacific

549   (30°S-30°N): -0.3-1.2%, north Pacific (45-65°N): 0.1-1.3%). In some regions, such as the

550 equatorial Pacific, NPP increases are balanced by decreases downstream, a result also

551 seen in other studies and suggested to be linked to macronutrient decreases downstream

552 from where iron fertilization occurs (Hamilton et al., 2020a; Ito et al., 2020b; Tagliabue et

553 al., 2008). Improved understanding of how variability in aerosol nutrient supply, over

554 different timescales, impacts ocean biogeochemistry requires a holistic multidisciplinary

555 approach, including consideration of: the physicochemical properties of different nutrient

556 aerosol sources; those interactions during atmospheric transport altering bioavailability;

557 mixing of aerosol nutrients from varied sources; and the multiple processes operating in

558 the surface mixed layer post-deposition.

559 **Summary Points**

560   1. Major nutrient sources include deserts/soils, wildfires, volcanoes, biogenic

561   particles, and industrial or vehicular pollution. Sources of nitrogen are strongly

562   linked to human activity while phosphate and soluble iron have considerable

563   natural sources.

564   2. Northern Hemisphere ocean nutrient fluxes are dominated by mineral dust sources

565   with an additional anthropogenic source at (sub-)polar latitudes. In the equatorial

566   Pacific and Southern Hemisphere oceans, fires are likely to be important.

567   3. Two-thirds of the iron in fires could be associated with dust particles entrained

568   within smoke plumes, although more work in needed to quantify this contribution.

569   Additionally, fires transform the landscape (soils and vegetation), creating a legacy

570   of secondary impacts altering nutrient aerosol supply until the ecosystem recovers.

571   4. In situ aerosol addition experiments suggest atmospheric deposition favors an

572   increase (~+80%) in Chl-a. However, in many experiments no response was

573   recorded and occasionally aerosols act as a pollutant or ballast decreasing Chl-a.

574   The characteristics of the receiving body of water, including its biota, is thus crucial

575   to understanding the impacts of changes to aerosol nutrient delivery.

576 5. At the global annual mean, modeling suggests fires have a net positive impact on

577   NPP (+0.7%). Regional increases can be higher (e.g., Southern Ocean: 0.7-1.3%)

578   and peak during the burning season (e.g., January-February Australian megafires

579   could have increased Southern Ocean NPP up to +3%).

580 6. A significant non-fire source of Australian soluble iron or mechanism increasing

581   the solubility of dust may be missing from atmospheric simulations of the iron cycle.

582 **Future Issues**

583 1. What are the mechanisms by which aerosol nutrients are distributed to oceans

584   under different climate regimes?

585 2. How does regional land use and climate change alter dust and (wild)fire activity,

586   both historically and in the future, and their roles in global biogeochemical cycles?

587 3. What field observations can aid in linking aerosol sources to observed

588   characteristics? Some suggestions include: Isotopes show promise in quantifying

589   human versus natural source contributions within mixed airmasses, but targeted

590   sampling on emissions from fires, forests, volcanoes, urban environments,

591   deserts, and mining operations are all essential; Time series stations can quantify

592   natural variability and the impact of long-term anthropogenic surface disturbances

593   as well as aid in extreme event attribution studies; Aircraft measurements taken

594   over marine regions compliment current ship-based observations to build a profile

595   of the distribution and changing properties of aerosol nutrients over their

596   atmospheric lifetime; In situ bioassay experiments are highly valuable, particularly

597   in unexplored key areas of the ocean.

598   4. How do differences in the physicochemical nature of different aerosol types alter

599   their interactions with a similarly diverse suite of oceanic physical, chemical, and

600   biological processes?

601   5. What is the response of net primary production and the biological pump to changes

602   in aerosol fluxes from different sources in the context of a changing ocean physical

603   state?

Acknowledgments

References

623 Altieri, K. E., Fawcett, S. E. and Hastings, M. G.: Reactive Nitrogen Cycling in the
624 Atmosphere and Ocean, Annu. Rev. Earth Planet. Sci., 49(1), 513–540,
625 doi:10.1146/annurev-earth-083120-052147, 2021.

626 Atanassova, I. and Doerr, S. H.: Changes in soil organic compound composition
627 associated with heat-induced increases in soil water repellency, Eur. J. Soil Sci., 62(4),
628 516–532, doi:10.1111/j.1365-2389.2011.01350.x, 2011.

629 Aumont, O., Ethé, C., Tagliabue, A., Bopp, L. and Gehlen, M.: PISCES-v2: An ocean
630 biogeochemical model for carbon and ecosystem studies, Geosci. Model Dev., 8(8),
631 2465–2513, doi:10.5194/gmd-8-2465-2015, 2015.

632 de Baar, H. J. W., Boyd, P. W., Coale, K. H., Landry, M. R., Tsuda, A., Assmy, P.,
633 Bakker, D. C. E., Bozec, Y., Barber, R. T., Brzezinski, M. A., Buesseler, K. O., Boyé, M.,
634 Croot, P. L., Gervais, F., Gorbunov, M. Y., Harrison, P. J., Hiscock, W. T., Laan, P.,
635 Lancelot, C., Law, C. S., Levasseur, M., Marchetti, A., Millero, F. J., Nishioka, J., Nojiri,
636 Y., van Oijen, T., Riebesell, U., Rijkenberg, M. J. A., Saito, H., Takeda, S.,
637 Timmermans, K. R., Veldhuis, M. J. W., Waite, A. M. and Wong, C. S.: Synthesis of iron
638 fertilization experiments: From the iron age in the age of enlightenment, J. Geophys.
639 Res. C Ocean., 110(9), 1–24, doi:10.1029/2004JC002601, 2005.

640 Baker, A. R. and Croot, P. L.: Atmospheric and marine controls on aerosol iron solubility
641 in seawater, Mar. Chem., 120(1–4), 4–13, doi:10.1016/j.marchem.2008.09.003, 2010.

642 Baker, A. R. and Jickells, T. D.: Atmospheric deposition of soluble trace elements along
643 the Atlantic Meridional Transect (AMT), Prog. Oceanogr., 158, 41–51,
644 doi:10.1016/j.pocean.2016.10.002, 2017.

645 Baker, A. R., Jickells, T. D., Biswas, K. F., Weston, K. and French, M.: Nutrients in
646 atmospheric aerosol particles along the Atlantic Meridional Transect, Deep Sea Res.
647 Part II Top. Stud. Oceanogr., 53(14–16), 1706–1719, doi:10.1016/j.dsr2.2006.05.012,
648 2006.

649 Baker, A. R., Weston, K., Kelly, S. D., Voss, M., Streu, P. and Cape, J. N.: Dry and wet
650 deposition of nutrients from the tropical Atlantic atmosphere: Links to primary
651 productivity and nitrogen fixation, Deep Sea Res. Part I Oceanogr. Res. Pap., 54(10),
652 1704–1720, doi:10.1016/j.dsr.2007.07.001, 2007.

653 Baker, A. R., Adams, C., Bell, T. G., Jickells, T. D. and Ganzeveld, L.: Estimation of
654 atmospheric nutrient inputs to the Atlantic Ocean from 50°N to 50°S based on large-
655 scale field sampling: Iron and other dust-associated elements, Global Biogeochem.

656   Cycles, 27(3), 755–767, doi:10.1002/gbc.20062, 2013.

657   Barkley, A. E., Prospero, J. M., Mahowald, N., Hamilton, D. S., Popendorf, K. J.,
658   Oehlert, A. M., Pourmand, A., Gatineau, A., Panechou-Pulcherie, K., Blackwelder, P.
659   and Gaston, C. J.: African biomass burning is a substantial source of phosphorus
660   deposition to the Amazon, Tropical Atlantic Ocean, and Southern Ocean, Proc. Natl.
661   Acad. Sci. U. S. A., 116(33), 16216–16221, doi:10.1073/pnas.1906091116, 2019.

662   Bhattarai, H., Saikawa, E., Wan, X., Zhu, H., Ram, K., Gao, S., Kang, S., Zhang, Q.,
663   Zhang, Y., Wu, G., Wang, X., Kawamura, K., Fu, P. and Cong, Z.: Levoglucosan as a
664   tracer of biomass burning: Recent progress and perspectives, Atmos. Res.,
665   220(September 2018), 20–33, doi:10.1016/j.atmosres.2019.01.004, 2019.

666   Boer, M. M., Resco de Dios, V. and Bradstock, R. A.: Unprecedented burn area of
667   Australian mega forest fires, Nat. Clim. Chang., 10(3), 171–172, doi:10.1038/s41558-
668   020-0716-1, 2020.

669   Bowie, A. R., Lannuzel, D., Remenyi, T. A., Wagener, T., Lam, P. J., Boyd, P. W.,
670   Guieu, C., Townsend, A. T. and Trull, T. W.: Biogeochemical iron budgets of the
671   Southern Ocean south of Australia: Decoupling of iron and nutrient cycles in the
672   subantarctic zone by the summertime supply, Global Biogeochem. Cycles, 23(4), 1–14,
673   doi:10.1029/2009GB003500, 2009.

674   Boyd, P. W. and Ellwood, M. J.: The biogeochemical cycle of iron in the ocean, Nat.
675   Geosci., 3(10), 675–682, doi:10.1038/ngeo964, 2010.

676   Boyd, P. W., Strzepek, R., Chiswell, S., Chang, H., DeBruyn, J. M., Ellwood, M.,
677   Keenan, S., King, A. L., Maas, E. W., Nodder, S., Sander, S. G., Sutton, P., Twining, B.
678   S., Wilhelm, S. W. and Hutchins, D. A.: Microbial control of diatom bloom dynamics in
679   the open ocean, Geophys. Res. Lett., 39(17), 2–7, doi:10.1029/2012GL053448, 2012.

680   Boyd, P. W., Strzepek, R. F., Ellwood, M. J., Hutchins, D. A., Nodder, S. D., Twining, B.
681   S. and Wilhelm, S. W.: Why are biotic iron pools uniform across high- and low-iron
682   pelagic ecosystems?, Global Biogeochem. Cycles, 29(7), 1028–1043,
683   doi:10.1002/2014GB005014, 2015.

684   Brahney, J., Mahowald, N., Ward, D. S., Ballantyne, A. P. and Neff, J. C.: Is
685   atmospheric phosphorus pollution altering global alpine Lake stoichiometry?, Global
686   Biogeochem. Cycles, 29(9), 1369–1383, doi:10.1002/2015GB005137, 2015.

687   Bressac, M. and Guieu, C.: Post-depositional processes: What really happens to new
688   atmospheric iron in the ocean's surface?, Global Biogeochem. Cycles, 27(3), 859–870,
689   doi:10.1002/gbc.20076, 2013.

690   Cao, F., Zhang, S. C., Kawamura, K., Liu, X., Yang, C., Xu, Z., Fan, M., Zhang, W.,
691   Bao, M., Chang, Y., Song, W., Liu, S., Lee, X., Li, J., Zhang, G. and Zhang, Y. L.:
692   Chemical characteristics of dicarboxylic acids and related organic compounds in PM2.5
693   during biomass-burning and non-biomass-burning seasons at a rural site of Northeast
694   China, Environ. Pollut., 231, 654–662, doi:10.1016/j.envpol.2017.08.045, 2017.

695   Capone, D., Zehr, J., Paerl, H., Bergman, B. and Carpenter, E.: Trichodesmium, a

696   globallly significant marine cyanobacterium, Science (80-.)., 276, 1221–1229, 1997.

697   Cassar, N., Bender, M. L., Barnett, B. A., Fan, S., Moxim, W. J., Levy, H. and Tilbrook,
698   B.: The southern ocean biological response to aeolian iron deposition, Science (80-.).,
699   317(5841), 1067–1070, doi:10.1126/science.1144602, 2007.

700   Chitrakar, R., Tezuka, S., Sonoda, A., Sakane, K., Ooi, K. and Hirotsu, T.: Phosphate
701   adsorption on synthetic goethite and akaganeite, J. Colloid Interface Sci., 298(2), 602–
702   608, doi:10.1016/j.jcis.2005.12.054, 2006.

703   Cong, Z., Kawamura, K., Kang, S. and Fu, P.: Penetration of biomass-burning
704   emissions from South Asia through the Himalayas: New insights from atmospheric
705   organic acids, Sci. Rep., 5, 1–7, doi:10.1038/srep09580, 2015.

706   Conway, T. M., Hamilton, D. S., Shelley, R. U., Aguilar-Islas, A. M., Landing, W. M.,
707   Mahowald, N. M. and John, S. G.: Tracing and constraining anthropogenic aerosol iron
708   fluxes to the North Atlantic Ocean using iron isotopes, Nat. Commun., 10(1),
709   doi:10.1038/s41467-019-10457-w, 2019.

710   Després, V. R., Alex Huffman, J., Burrows, S. M., Hoose, C., Safatov, A. S., Buryak, G.,
711   Fröhlich-Nowoisky, J., Elbert, W., Andreae, M. O., Pöschl, U. and Jaenicke, R.: Primary
712   biological aerosol particles in the atmosphere: A review, Tellus, Ser. B Chem. Phys.
713   Meteorol., 64(1), doi:10.3402/tellusb.v64i0.15598, 2012.

714   Doney, S. C., Lima, I., Feely, R. A., Glover, D. M., Lindsay, K., Mahowald, N., Moore, J.
715   K. and Wanninkhof, R.: Mechanisms governing interannual variability in upper-ocean
716   inorganic carbon system and air-sea CO2 fluxes: Physical climate and atmospheric
717   dust, Deep. Res. Part II Top. Stud. Oceanogr., 56(8–10), 640–655,
718   doi:10.1016/j.dsr2.2008.12.006, 2009.

719   Dowdy, A. J., Ye, H., Pepler, A., Thatcher, M., Osbrough, S. L., Evans, J. P., Di Virgilio,
720   G. and McCarthy, N.: Future changes in extreme weather and pyroconvection risk
721   factors for Australian wildfires, Sci. Rep., 9(1), 1–11, doi:10.1038/s41598-019-46362-x,
722   2019.

723   Duce, R. A., Liss, P. S., Merrill, J. T., Atlas, E. L., Buat-Menard, P., Hicks, B. B., Miller,
724   J. M., Prospero, J. M., Arimoto, R., Church, T. M., Ellis, W., Galloway, J. N., Hansen, L.,
725   Jickells, T. D., Knap, A. H., Reinhardt, K. H., Schneider, B., Soudine, A., Tokos, J. .,
726   Tsunogai, S., Wollast, R. and Zhou, M.: The atmospheric input of trace species to the
727   world ocean., Global Biogeochem. Cycles, 5(3), 193–259, 1991.

728   Duggen, S., Croot, P., Schacht, U. and Hoffmann, L.: Subduction zone volcanic ash can
729   fertilize the surface ocean and stimulate phytoplankton growth: Evidence from
730   biogeochemical experiments and satellite data, Geophys. Res. Lett., 34(1), L01612,
731   doi:10.1029/2006GL027522, 2007.

732   Duggen, S., Olgun, N., Croot, P., Hoffmann, L., Dietze, H., Delmelle, P. and Teschner,
733   C.: The role of airborne volcanic ash for the surface ocean biogeochemical iron-cycle: a
734   review, Biogeosciences, 7(3), 827–844, doi:10.5194/bg-7-827-2010, 2010.

735   Dukes, D., Gonzales, H. B., Ravi, S., Grandstaff, D. E., Van Pelt, R. S., Li, J., Wang, G.

736   and Sankey, J. B.: Quantifying Postfire Aeolian Sediment Transport Using Rare Earth
737   Element Tracers, J. Geophys. Res. Biogeosciences, 123(1), 288–299,
738   doi:10.1002/2017JG004284, 2018.

739   Fishwick, M. P., Sedwick, P. N., Lohan, M. C., Worsfold, P. J., Buck, K. N., Church, T.
740   M. and Ussher, S. J.: The impact of changing surface ocean conditions on the
741   dissolution of aerosol iron, Global Biogeochem. Cycles, 28(11), 1235–1250,
742   doi:10.1002/2014GB004921, 2014.

743   Fung, I., Meyn, S. K., Tegen, I., Doney, S., John, J. and Bishop, J.: Iron supply and
744   demand in the upper ocean, Global Biogeochem. Cycles, 14(1), 281–295, 2000.

745   Gabric, A. J., Cropp, R. A., McTainsh, G. H., Johnston, B. M., Butler, H., Tilbrook, B.
746   and Keywood, M.: Australian dust storms in 2002-2003 and their impact on Southern
747   Ocean biogeochemistry, Global Biogeochem. Cycles, 24(2),
748   doi:10.1029/2009GB003541, 2010.

749   Gaudichet, A., Echalar, F., Chatenet, B., Quisefit, J. P., Malingre, G., Cachier, H., Buat-
750   Menard, P., Artaxo, P. and Maenhaut, W.: Trace elements in tropical African savanna
751   biomass burning aerosols, J. Atmos. Chem., 22(1–2), 19–39, doi:10.1007/BF00708179,
752   1995.

753   Gazeau, F., Ridame, C., Van Wambeke, F., Alliouane, S., Stolpe, C., Irisson, J.-O.,
754   Marro, S., Grisoni, J.-M., De Liège, G., Nunige, S., Djaoudi, K., Pulido-Villena, E.,
755   Dinasquet, J., Obernosterer, I., Catala, P. and Guieu, C.: Impact of dust enrichment on
756   Mediterranean plankton communities under present and future conditions of pH and
757   temperature: an experimental overview, Biogeosciences Discuss., 21(1), 1–81,
758   doi:10.5194/bg-2020-202, 2020.

759   Geng, H., Park, Y., Hwang, H., Kang, S. and Ro, C. U.: Elevated nitrogen-containing
760   particles observed in Asian dust aerosol samples collected at the marine boundary layer
761   of the Bohai Sea and the Yellow Sea, Atmos. Chem. Phys., 9(18), 6933–6947,
762   doi:10.5194/acp-9-6933-2009, 2009.

763   Ginoux, P., Prospero, J. M., Gill, T. E., Hsu, N. C. and Zhao, M.: Global-scale attribution
764   of anthropogenic and natural dust sources and their emission rates based on MODIS
765   Deep Blue aerosol products, Rev. Geophys., 50(3), 1–36, doi:10.1029/2012RG000388,
766   2012.

767   Giovagnetti, V., Brunet, C., Conversano, F., Tramontano, F., Obernosterer, I., Ridame,
768   C. and Guieu, C.: Assessing the role of dust deposition on phytoplankton ecophysiology
769   and succession in a low-nutrient low-chlorophyll ecosystem: A mesocosm experiment in
770   the mediterranean sea, Biogeosciences, 10(5), 2973–2991, doi:10.5194/bg-10-2973-
771   2013, 2013.

772   Graham, B., Guyon, P., Maenhaut, W., Taylor, P. E., Ebert, M., Matthias-Maser, S.,
773   Mayol-Bracero, O. L., Godoi, R. H. M., Artaxo, P., Meixner, F. X., Moura, M. a. L.,
774   Rocha, C. H. E. D., Grieken, R. Van, Glovsky, M. M., Flagan, R. C. and Andreae, M. O.:
775   Composition and diurnal variability of the natural Amazonian aerosol, J. Geophys. Res.
776   Atmos., 108(D24), n/a-n/a, doi:10.1029/2003JD004049, 2003.

Guieu, C., Bonnet, S., Wagener, T. and Loÿe-Pilot, M. D.: Biomass burning as a source of dissolved iron to the open ocean?, Geophys. Res. Lett., 32(L19608), 1–5, doi:10.1029/2005GL022962, 2005.

Guieu, C., Dulac, F., Desboeufs, K., Wagener, T., Pulido-Villena, E., Grisoni, J. M., Louis, F., Ridame, C., Blain, S., Brunet, C., Bon Nguyen, E., Tran, S., Labiadh, M. and Dominici, J. M.: Large clean mesocosms and simulated dust deposition: A new methodology to investigate responses of marine oligotrophic ecosystems to atmospheric inputs, Biogeosciences, 7(9), 2765–2784, doi:10.5194/bg-7-2765-2010, 2010.

Guieu, C., Ridame, C., Pulido-Villena, E., Bressac, M., Desboeufs, K. and Dulac, F.: Impact of dust deposition on carbon budget: A tentative assessment from a mesocosm approach, Biogeosciences, 11(19), 5621–5635, doi:10.5194/bg-11-5621-2014, 2014a.

Guieu, C., Aumont, O., Paytan, A., Bopp, L., Law, C. S., Mahowald, N., Achterberg, E. P., Marañón, E., Salihoglu, B., Crise, A., Wagener, T., Herut, B., Desboeufs, K., Kanakidou, M., Olgun, N., Peters, F., Pulido-Villena, E., Tovar-Sanchez, A. and Völker, C.: The significance of the episodic nature of atmospheric deposition to Low Nutrient Low Chlorophyll regions, Global Biogeochem. Cycles, 28(11), 1179–1198, doi:10.1002/2014GB004852, 2014b.

Guieu, C., Al Azhar, M., Aumont, O., Mahowald, N., Levy, M., Ethé, C. and Lachkar, Z.: Major Impact of Dust Deposition on the Productivity of the Arabian Sea, Geophys. Res. Lett., 46(12), 6736–6744, doi:10.1029/2019GL082770, 2019.

Hamilton, D. S., Lee, L. A., Pringle, K. J., Reddington, C. L., Spracklen, D. V and Carslaw, K. S.: Occurrence of pristine aerosol environments on a polluted planet., Proc. Natl. Acad. Sci. U. S. A., 111(52), 18466–71, doi:10.1073/pnas.1415440111, 2014.

Hamilton, D. S., Hantson, S., Scott, C. E., Kaplan, J. O., Pringle, K. J., Nieradzik, L. P., Rap, A., Folberth, G. A., Spracklen, D. V. and Carslaw, K. S.: Reassessment of pre-industrial fire emissions strongly affects anthropogenic aerosol forcing, Nat. Commun., 9(1), 3182, doi:10.1038/s41467-018-05592-9, 2018.

Hamilton, D. S., Scanza, R. A., Feng, Y., Guinness, J., Kok, J. F., Li, L., Liu, X., Rathod, S. D., Wan, J. S., Wu, M. and Mahowald, N. M.: Improved methodologies for Earth system modelling of atmospheric soluble iron and observation comparisons using the Mechanism of Intermediate complexity for Modelling Iron (MIMI v1.0), Geosci. Model Dev., 12(9), 3835–3862, doi:10.5194/gmd-12-3835-2019, 2019.

Hamilton, D. S., Moore, J. K., Arneth, A., Bond, T. C., Carslaw, K. S., Hantson, S., Ito, A., Kaplan, J. O., Lindsay, K., Nieradzik, L., Rathod, S. D., Scanza, R. A. and Mahowald, N. M.: Impact of Changes to the Atmospheric Soluble Iron Deposition Flux on Ocean Biogeochemical Cycles in the Anthropocene, Global Biogeochem. Cycles, 34(3), 1–22, doi:10.1029/2019GB006448, 2020a.

Hamilton, D. S., Scanza, R. A., Rathod, S. D., Bond, T. C., Kok, J. F., Li, L., Matsui, H. and Mahowald, N. M.: Recent (1980 to 2015) Trends and Variability in Daily-to-Interannual Soluble Iron Deposition from Dust, Fire, and Anthropogenic Sources,

818   Geophys. Res. Lett., 47(17), e2020GL089688, doi:10.1029/2020GL089688, 2020b.

819   Herbert, R. J., Krom, M. D., Carslaw, K. S., Stockdale, A., Mortimer, R. J. G., Benning,
820   L. G., Pringle, K. and Browse, J.: The Effect of Atmospheric Acid Processing on the
821   Global Deposition of Bioavailable Phosphorus From Dust, Global Biogeochem. Cycles,
822   32(9), 1367–1385, doi:10.1029/2018GB005880, 2018.

823   Hoffmann, L. J., Breitbarth, E., Ardelan, M. V., Duggen, S., Olgun, N., Hasseliöv, M. and
824   Wängberg, S. Å.: Influence of trace metal release from volcanic ash on growth of
825   Thalassiosira pseudonana and Emiliania huxleyi, Mar. Chem., 132–133, 28–33,
826   doi:10.1016/j.marchem.2012.02.003, 2012.

827   Ito, A.: Atmospheric processing of combustion aerosols as a source of bioavailable iron,
828   Environ. Sci. Technol. Lett., 2(3), 70–75, doi:10.1021/acs.estlett.5b00007, 2015.

829   Ito, A. and Shi, Z.: Delivery of anthropogenic bioavailable iron from mineral dust and
830   combustion aerosols to the ocean, Atmos. Chem. Phys., 16(1), 85–99, doi:10.5194/acp-
831   16-85-2016, 2016.

832   Ito, A., Myriokefalitakis, S., Kanakidou, M., Mahowald, N. M., Scanza, R. A., Hamilton,
833   D. S., Baker, A. R., Jickells, T., Sarin, M., Bikkina, S., Gao, Y., Shelley, R. U., Buck, C.
834   S., Landing, W. M., Bowie, A. R., Perron, M. M. G., Guieu, C., Meskhidze, N., Johnson,
835   M. S., Feng, Y., Kok, J. F., Nenes, A. and Duce, R. A.: Pyrogenic iron: The missing link
836   to high iron solubility in aerosols, Sci. Adv., 5(5), 1–10, doi:10.1126/sciadv.aau7671,
837   2019.

838   Ito, A., Perron, M. M. G., Proemse, B. C., Strzelec, M., Gault-Ringold, M., Boyd, P. W.
839   and Bowie, A. R.: Evaluation of aerosol iron solubility over Australian coastal regions
840   based on inverse modeling: implications of bushfires on bioaccessible iron
841   concentrations in the Southern Hemisphere, Prog. Earth Planet. Sci., 7(1),
842   doi:10.1186/s40645-020-00357-9, 2020a.

843   Ito, A., Ye, Y., Yamamoto, A., Watanabe, M. and Aita, M. N.: Responses of ocean
844   biogeochemistry to atmospheric supply of lithogenic and pyrogenic iron-containing
845   aerosols, Geol. Mag., 1–16, doi:10.1017/S0016756819001080, 2020b.

846   Ito, A., Adebiyi, A. A., Huang, Y. and Kok, J. F.: Less atmospheric radiative heating due
847   to aspherical dust with coarser size, Atmos. Chem. Phys. Discuss., (February), 1–44,
848   doi:10.5194/acp-2021-134, 2021.

849   Jaenicke, R., Matthias-Maser, S. and Gruber, S.: Omnipresence of biological material in
850   the atmosphere, Environ. Chem., 4(4), 217–220, doi:10.1071/EN07021, 2007.

851   Jeanneau, A. C., Ostendorf, B. and Herrmann, T.: Relative spatial differences in
852   sediment transport in fire-affected agricultural landscapes: A field study, Aeolian Res.,
853   39(December 2018), 13–22, doi:10.1016/j.aeolia.2019.04.002, 2019.

854   Jickells, T. D., An, Z. S., Andersen, K. K., Baker, A. R., Bergametti, G., Brooks, N., Cao,
855   J. J., Boyd, P. W., Duce, R. A., Hunter, K. A., Kawahata, H., Kubilay, N., LaRoche, J.,
856   Liss, P. S., Mahowald, N., Prospero, J. M., Ridgwell, a J., Tegen, I. and Torres, R.:
857   Global iron connections between desert dust, ocean biogeochemistry, and climate.,

858   Science, 308(5718), 67–71, doi:10.1126/science.1105959, 2005.

859   Jickells, T. D., Buitenhuis, E., Altieri, K., Baker, A. R., Capone, D., Duce, R. A.,
860   Dentener, F., Fennel, K., Kanakidou, M., LaRoche, J., Lee, K., Liss, P., Middelburg, J.
861   J., Moore, J. K., Okin, G., Oschlies, A., Sarin, M., Seitzinger, S., Sharples, J., Singh, A.,
862   Suntharalingam, P., Uematsu, M. and Zamora, L. M.: A reevaluation of the magnitude
863   and impacts of anthropogenic atmospheric nitrogen inputs on the ocean, Global
864   Biogeochem. Cycles, 31(2), 289–305, doi:10.1002/2016GB005586, 2017.

865   Johnson, M. S. and Meskhidze, N.: Atmospheric dissolved iron deposition to the global
866   oceans: Effects of oxalate-promoted Fe dissolution, photochemical redox cycling, and
867   dust mineralogy, Geosci. Model Dev., 6(4), 1137–1155, doi:10.5194/gmd-6-1137-2013,
868   2013.

869   Journet, E., Desbouefs, K., Caqineau, S. and Colin, J.-L.: Mineralogy as a critical factor
870   of dust iron solubility, Geophys. Res. Lett., 35(L07805), doi:10.1029/2007GL031589,
871   2008.

872   Journet, E., Balkanski, Y. and Harrison, S. P.: A new data set of soil mineralogy for
873   dust-cycle modeling, Atmos. Chem. Phys., 14(8), 3801–3816, doi:10.5194/acp-14-3801-
874   2014, 2014.

875   Kanakidou, M., Duce, R. a., Prospero, J. M., Baker, A. R., Benitez-Nelson, C.,
876   Dentener, F. J., Hunter, K. a., Liss, P. S., Mahowald, N., Okin, G. S., Sarin, M.,
877   Tsigaridis, K., Uematsu, M., Zamora, L. M. and Zhu, T.: Atmospheric fluxes of organic N
878   and P to the global ocean, Global Biogeochem. Cycles, 26(3), n/a-n/a,
879   doi:10.1029/2011GB004277, 2012.

880   Kanakidou, M., Myriokefalitakis, S., Daskalakis, N., Fanourgakis, G., Nenes, A., Baker,
881   A. R., Tsigaridis, K. and Mihalopoulos, N.: Past, present, and future atmospheric
882   nitrogen deposition, J. Atmos. Sci., 73(5), 2039–2047, doi:10.1175/JAS-D-15-0278.1,
883   2016.

884   Kanakidou, M., Myriokefalitakis, S. and Tsigaridis, K.: Aerosols in atmospheric
885   chemistry and biogeochemical cycles of nutrients, Environ. Res. Lett., 13(6),
886   doi:10.1088/1748-9326/aabcdb, 2018.

887   Kavouras, I. G., Nikolich, G., Etyemezian, V., Dubois, D. W., King, J. and Shafer, D.: In
888   situ observations of soil minerals and organic matter in the early phases of prescribed
889   fires, J. Geophys. Res. Atmos., 117(12), 1–9, doi:10.1029/2011JD017420, 2012.

890   Khaykin, S., Legras, B., Bucci, S., Sellitto, P., Isaksen, L., Tencé, F., Bekki, S.,
891   Bourassa, A., Rieger, L., Zawada, D., Jumelet, J. and Godin-Beekmann, S.: The
892   2019/20 Australian wildfires generated a persistent smoke-charged vortex rising up to
893   35 km altitude, Commun. Earth Environ., 1(1), 1–12, doi:10.1038/s43247-020-00022-5,
894   2020.

895   Kok, J. F., Adebiyi, A. A., Albani, S., Balkanski, Y., Checa-garcia, R., Colarco, P. R.,
896   Hamilton, D. S., Huang, Y., Ito, A., Klose, M., Li, L., Mahowald, N. M., Miller, R. L.,
897   Obiso, V., García-pando, C. P., Rocha-Lima, A. and Wan, J. S.: Contribution of the
898   world's main dust source regions to the global cycle of desert dust, Atmos. Chem. Phys.

899 Discuss., (January), 1–34, doi:10.5194/acp-2021-4, 2021.

900 Krishnamurthy, A., Moore, J. K., Mahowald, N., Luo, C., Doney, S. C., Lindsay, K. and
901 Zender, C. S.: Impacts of increasing anthropogenic soluble iron and nitrogen deposition
902 on ocean biogeochemistry, Global Biogeochem. Cycles, 23(3), 1–15,
903 doi:10.1029/2008GB003440, 2009.

904 Kundu, S., Kawamura, K., Andreae, T. W., Hoffer, A. and Andreae, M. O.: Diurnal
905 variation in the water-soluble inorganic ions, organic carbon and isotopic compositions
906 of total carbon and nitrogen in biomass burning aerosols from the LBA-SMOCC
907 campaign in Rondônia, Brazil, J. Aerosol Sci., 41(1), 118–133,
908 doi:10.1016/j.jaerosci.2009.08.006, 2010.

909 Lamb, K. D., Matsui, H., Katich, J. M., Perring, A. E., Spackman, J. R., Weinzierl, B.,
910 Dollner, M. and Schwarz, J. P.: Global-scale constraints on light-absorbing
911 anthropogenic iron oxide aerosols, npj Clim. Atmos. Sci., 4(1), 15, doi:10.1038/s41612-
912 021-00171-0, 2021.

913 Langmann, B.: Volcanic Ash versus Mineral Dust: Atmospheric Processing and
914 Environmental and Climate Impacts, ISRN Atmos. Sci., 2013, 1–17,
915 doi:10.1155/2013/245076, 2013.

916 Lasaga, A. C., Soler, J. M., Ganor, J., Burch, T. E. and Nagy, K. L.: Chemical
917 weathering rate laws and global geochemical cycles, Geochim. Cosmochim. Acta,
918 58(10), 2361–2386, doi:10.1016/0016-7037(94)90016-7, 1994.

919 Letelier, R. M., Björkman, K. M., Church, M. J., Hamilton, D. S., Mahowald, N. M.,
920 Scanza, R. A., Schneider, N., White, A. E. and Karl, D. M.: Climate-driven oscillation of
921 phosphorus and iron limitation in the North Pacific Subtropical Gyre, Proc. Natl. Acad.
922 Sci. U. S. A., 116(26), 12720–12728, doi:10.1073/pnas.1900789116, 2019.

923 Li, W., Xu, L., Liu, X., Zhang, J., Lin, Y., Yao, X., Gao, H., Zhang, D., Chen, J., Wang,
924 W. and Harrison, R. M.: Air pollution – aerosol interactions produce more bioavailable
925 iron for ocean ecosystems, Sci. Adv., (March), 1–7, doi:10.1126/sciadv.1601749, 2017.

926 Longo, A. F., Feng, Y., Lai, B., Landing, W. M., Shelley, R. U., Nenes, A., Mihalopoulos,
927 N., Violaki, K. and Ingall, E. D.: Influence of Atmospheric Processes on the Solubility
928 and Composition of Iron in Saharan Dust, Environ. Sci. Technol., 50(13), 6912–6920,
929 doi:10.1021/acs.est.6b02605, 2016.

930 Louis, J., Bressac, M., Pedrotti, M. L. and Guieu, C.: Dissolved inorganic nitrogen and
931 phosphorus dynamics in seawater following an artificial Saharan dust deposition event,
932 Front. Mar. Sci., 2(MAY), 1–11, doi:10.3389/fmars.2015.00027, 2015.

933 Louis, J., Gazeau, F. and Guieu, C.: Atmospheric nutrients in seawater under current
934 and high pCO2 conditions after Saharan dust deposition: Results from three minicosm
935 experiments, Prog. Oceanogr., 163(October 2017), 40–49,
936 doi:10.1016/j.pocean.2017.10.011, 2018.

937 Luo, C., Mahowald, N., Bond, T., Chuang, P. Y., Artaxo, P., Siefert, R., Chen, Y. and
938 Schauer, J.: Combustion iron distribution and deposition, Global Biogeochem. Cycles,

939   22(GB1012), 1–17, doi:10.1029/2007GB002964, 2008.

940   Mackie, D. S., Boyd, P. W., McTainsh, G. H., Tindale, N. W., Westberry, T. K. and
941   Hunter, K. A.: Biogeochemistry of iron in Australian dust: From eolian uplift to marine
942   uptake, Geochemistry, Geophys. Geosystems, 9(3), doi:10.1029/2007GC001813, 2008.

943   Maenhaut, W., Salma, I., Cafmeyer, J., Annegarn, H. J. and Andreae, M. O.: Regional
944   atmospheric aerosol composition and sources in the eastern Transvaal, South Africa,
945   and impact of biomass burning, J. Geophys. Res. Atmos., 101(19), 23631–23650,
946   doi:10.1029/95jd02930, 1996.

947   Mahowald, N., Jickells, T. D., Baker, A. R., Artaxo, P., Benitez-Nelson, C. R.,
948   Bergametti, G., Bond, T. C., Chen, Y., Cohen, D. D., Herut, B., Kubilay, N., Losno, R.,
949   Luo, C., Maenhaut, W., McGee, K. A., Okin, G. S., Siefert, R. L. and Tsukuda, S.:
950   Global distribution of atmospheric phosphorus sources, concentrations and deposition
951   rates, and anthropogenic impacts, Global Biogeochem. Cycles, 22(4), 1–19,
952   doi:10.1029/2008GB003240, 2008.

953   Mahowald, N. M., Artaxo, P., Baker, A. R., Jickells, T. D., Okin, G. S., Randerson, J. T.
954   and Townsend, A. R.: Impacts of biomass burning emissions and land use change on
955   Amazonian atmospheric phosphorus cycling and deposition, Global Biogeochem.
956   Cycles, 19(4), doi:10.1029/2005GB002541, 2005.

957   Mahowald, N. M., Engelstaedter, S., Luo, C., Sealy, A., Artaxo, P., Benitez-Nelson, C.,
958   Bonnet, S., Chen, Y., Chuang, P. Y., Cohen, D. D., Dulac, F., Herut, B., Johansen, A.
959   M., Kubilay, N., Losno, R., Maenhaut, W., Paytan, A., Prospero, J. M., Shank, L. M. and
960   Siefert, R. L.: Atmospheric iron deposition: global distribution, variability, and human
961   perturbations., Ann. Rev. Mar. Sci., 1, 245–278,
962   doi:10.1146/annurev.marine.010908.163727, 2009.

963   Mahowald, N. M., Kloster, S., Engelstaedter, S., Moore, J. K., Mukhopadhyay, S.,
964   McConnell, J. R., Albani, S., Doney, S. C., Bhattacharya, A., Curran, M. A. J., Flanner,
965   M. G., Hoffman, F. M., Lawrence, D. M., Lindsay, K., Mayewski, P. A., Neff, J.,
966   Rothenberg, D., Thomas, E., Thornton, P. E. and Zender, C. S.: Observed 20th century
967   desert dust variability: Impact on climate and biogeochemistry, Atmos. Chem. Phys.,
968   10(22), 10875–10893, doi:10.5194/acp-10-10875-2010, 2010.

969   Mahowald, N. M., Hamilton, D. S., Mackey, K. R. M., Moore, J. K., Baker, A. R.,
970   Scanza, R. A. and Zhang, Y.: Aerosol trace metal leaching and impacts on marine
971   microorganisms, Nat. Commun., 9(1), 2614, doi:10.1038/s41467-018-04970-7, 2018.

972   Marañón, E., Fernández, A., Mouriño-Carballido, B., Martínez-García, S., Teira, E.,
973   Cermeño, P., Chouciño, P., Huete-Ortega, M., Fernández, E., Calvo-Díaz, A., Morán, X.
974   A. G., Bode, A., Moreno-Ostos, E., Varela, M. M., Patey, M. D. and Achterberg, E. P.:
975   Degree of oligotrophy controls the response of microbial plankton to Saharan dust,
976   Limnol. Oceanogr., 55(6), 2339–2352, doi:10.4319/lo.2010.55.6.2339, 2010.

977   Martin, H., Gordon, R. M. and Fitzwater, S. E.: The case for iron, Limnol. Ocean., 36(8),
978   1793–1802, 1991.

979   Martin, J.: Glacial-interglacial CO2 change: The iron hypothesis, Paleoceanography,

980   5(1), 1–13, 1990.

981   Matsui, H., Mahowald, N. M., Moteki, N., Hamilton, D. S., Ohata, S., Yoshida, A., Koike,
982   M., Scanza, R. A. and Flanner, M. G.: Anthropogenic combustion iron as a complex
983   climate forcer, Nat. Commun., 9(1), 1–10, doi:10.1038/s41467-018-03997-0, 2018.

984   McLennan, S. M.: Relationships between the trace element composition of sedimentary
985   rocks and upper continental crust, Geochemistry, Geophys. Geosystems, 2(4),
986   2000GC000109, doi:10.1029/2000GC000109, 2001.

987   McNabb, D. H. and Swanson, F. J.: Effects of fire on soil erosion, in Natural and
988   Prescribed Fire in Pacific Northwest Forests, pp. 159–176., 1990.

989   Meskhidze, N., Chameides, W. L. and Nenes, A.: Dust and pollution: A recipe for
990   enhanced ocean fertilization?, J. Geophys. Res. Atmos., 110(D03301), 1–23,
991   doi:10.1029/2004JD005082, 2005.

992   Moore, C. M. M., Mills, M. M. M., Arrigo, K. R. R., Berman-Frank, I., Bopp, L., Boyd, P.
993   W. W., Galbraith, E. D. D., Geider, R. J. J., Guieu, C., Jaccard, S. L. L., Jickells, T. D.
994   D., La Roche, J., Lenton, T. M. M., Mahowald, N. M. M., Marañón, E., Marinov, I.,
995   Moore, J. K. K., Nakatsuka, T., Oschlies, A., Saito, M. A. A., Thingstad, T. F. F., Tsuda,
996   A. and Ulloa, O.: Processes and patterns of oceanic nutrient limitation, Nat. Geosci.,
997   6(9), 701–710, doi:10.1038/ngeo1765, 2013.

998   Myriokefalitakis, S., Tsigaridis, K., Mihalopoulos, N., Sciare, J., Nenes, A., Kawamura,
999   K., Segers, A. and Kanakidou, M.: In-cloud oxalate formation in the global troposphere:
1000   A 3-D modeling study, Atmos. Chem. Phys., 11(12), 5761–5782, doi:10.5194/acp-11-
1001   5761-2011, 2011.

1002   Myriokefalitakis, S., Daskalakis, N., Mihalopoulos, N., Baker, A. R., Nenes, A. and
1003   Kanakidou, M.: Changes in dissolved iron deposition to the oceans driven by human
1004   activity: a 3-D global modelling study, Biogeosciences, 12(13), 3973–3992,
1005   doi:10.5194/bg-12-3973-2015, 2015.

1006   Myriokefalitakis, S., Nenes, A., Baker, A. R., Mihalopoulos, N. and Kanakidou, M.:
1007   Bioavailable atmospheric phosphorous supply to the global ocean: A 3-D global
1008   modeling study, Biogeosciences, 13(24), 6519–6543, doi:10.5194/bg-13-6519-2016,
1009   2016.

1010   Myriokefalitakis, S., Ito, A., Kanakidou, M., Nenes, A., Krol, M. C., Mahowald, N. M.,
1011   Scanza, R. A., Hamilton, D. S., Johnson, M. S., Meskhidze, N., Kok, J. F., Guieu, C.,
1012   Baker, A. R., Jickells, T. D., Sarin, M. M., Bikkina, S., Shelley, R., Bowie, A., Perron, M.
1013   M. G. and Duce, R. A.: Reviews and syntheses: The GESAMP atmospheric iron
1014   deposition model intercomparison study, Biogeosciences, 15(21), 6659–6684,
1015   doi:10.5194/bg-15-6659-2018, 2018.

1016   Myriokefalitakis, S., Gröger, M., Hieronymus, J. and Döscher, R.: An explicit estimate of
1017   the atmospheric nutrient impact on global oceanic productivity, Ocean Sci., 16(5),
1018   1183–1205, doi:10.5194/os-16-1183-2020, 2020.

1019   Nenes, A., Krom, M. D., Mihalopoulos, N., Van Cappellen, P., Shi, Z., Bougiatioti, A.,

Zarmpas, P. and Herut, B.: Atmospheric acidification of mineral aerosols: A source of bioavailable phosphorus for the oceans, Atmos. Chem. Phys., 11(13), 6265–6272, doi:10.5194/acp-11-6265-2011, 2011.

Nisantzi, A., Mamouri, R. E., Ansmann, A. and Hadjimitsis, D.: Injection of mineral dust into the free troposphere during fire events observed with polarization lidar at Limassol, Cyprus, Atmos. Chem. Phys., 14(22), 12155–12165, doi:10.5194/acp-14-12155-2014, 2014.

Oakes, M., Ingall, E. D., Lai, B., Shafer, M. M., Hays, M. D., Liu, Z. G., Russell, A. G. and Weber, R. J.: Iron solubility related to particle sulfur content in source emission and ambient fine particles, Environ. Sci. Technol., 46(12), 6637–6644, doi:10.1021/es300701c, 2012.

Olgun, N., Duggen, S., Croot, P. L., Delmelle, P., Dietze, H., Schacht, U., Óskarsson, N., Siebe, C., Auer, A. and Garbe-Schönberg, D.: Surface ocean iron fertilization: The role of airborne volcanic ash from subduction zone and hot spot volcanoes and related iron fluxes into the Pacific Ocean, Global Biogeochem. Cycles, 25(GB4001), 1–15, doi:10.1029/2009GB003761, 2011.

Olgun, N., Duggen, S., Andronico, D., Kutterolf, S., Croot, P. L., Giammanco, S., Censi, P. and Randazzo, L.: Possible impacts of volcanic ash emissions of Mount Etna on the primary productivity in the oligotrophic Mediterranean Sea: Results from nutrient-release experiments in seawater, Mar. Chem., 152, 32–42, doi:10.1016/j.marchem.2013.04.004, 2013.

Parekh, P., Follows, M. J. and Boyle, E.: Modeling the global ocean iron cycle, Global Biogeochem. Cycles, 18(1), n/a-n/a, doi:10.1029/2003gb002061, 2004.

Paris, R., Desboeufs, K. V., Formenti, P., Nava, S. and Chou, C.: Chemical characterisation of iron in dust and biomass burning aerosols during AMMA-SOP0/DABEX: Implication for iron solubility, Atmos. Chem. Phys., 10(9), 4273–4282, doi:10.5194/acp-10-4273-2010, 2010.

Paytan, A., Mackeya, K. R. M., Chena, Y., Limac, I. D., Doney, S. C. S. C., Mahowald, N., Labiosae, R., Post, A. F. A. F., Paytan, A., Mackey, K. R. M., Chen, Y., Lima, I. D., Doney, S. C. S. C., Mahowald, N., Labiosa, R. and Post, A. F. A. F.: Toxicity of atmospheric aerosols on marine phytoplankton., Proc. Natl. Acad. Sci. U. S. A., 106(12), 4601–4605, doi:10.1073/pnas.0811486106, 2009.

Pérez-Cabello, F., de la Riva Fernández, J., Montorio Llovería, R. and García-Martín, A.: Mapping erosion-sensitive areas after wildfires using fieldwork, remote sensing, and geographic information systems techniques on a regional scale, J. Geophys. Res. Biogeosciences, 111(4), 1–13, doi:10.1029/2005JG000148, 2006.

Perron, M. M. G., Proemse, B. C., Strzelec, M., Gault-Ringold, M., Boyd, P. W., Rodriguez, E. S., Paull, B. and Bowie, A. R.: Origin, transport and deposition of aerosol iron to Australian coastal waters, Atmos. Environ., 228(October 2019), 117432, doi:10.1016/j.atmosenv.2020.117432, 2020.

Ramos, M. E., Garcia-Palma, S., Rozalen, M., Johnston, C. T. and Huertas, F. J.:

1061   Kinetics of montmorillonite dissolution. An experimental study of the effect of oxalate.,
1062   Chem. Geol., 363, 283–292, doi:10.1016/j.chemgeo.2013.11.014, 2014.

1063   Rathod, S. D., Hamilton, D. S., Mahowald, N. M., Klimont, Z., Corbett, J. J. and Bond, T.
1064   C.: A mineralogy-based anthropogenic combustion-iron emission inventory, J. Geophys.
1065   Res. Atmos., 125(17), e2019JD032114, doi:10.1029/2019jd032114, 2020.

1066   Reid, J. S., Koppmann, R., Eck, T. F. and Eleuterio, D. P.: A review of biomass burning
1067   emissions part II: intensive physical properties of biomass burning particles, Atmos.
1068   Chem. Phys., 5, 799–825, 2005.

1069   La Roche, J. and Breitbarth, E.: Importance of the diazotrophs as a source of new
1070   nitrogen in the ocean, J. Sea Res., 53(1-2 SPEC. ISS.), 67–91,
1071   doi:10.1016/j.seares.2004.05.005, 2005.

1072   Sarmiento, J. L., Gruber, N., Brzezinski, M. A. and Dunne, J. P.: High-latitude controls
1073   of thermocline nutrients and low latitude biological productivity, Nature, 427(6969), 56–
1074   60, doi:10.1038/nature02127, 2004.

1075   Schlosser, J. S., Braun, R. A., Bradley, T., Dadashazar, H., MacDonald, A. B., Aldhaif,
1076   A. A., Aghdam, M. A., Mardi, A. H., Xian, P. and Sorooshian, A.: Analysis of aerosol
1077   composition data for western United States wildfires between 2005 and 2015: Dust
1078   emissions, chloride depletion, and most enhanced aerosol constituents, J. Geophys.
1079   Res. Atmos., 122(16), 8951–8966, doi:10.1002/2017JD026547, 2017.

1080   Schmidl, C., Marr, I. L., Caseiro, A., Kotianová, P., Berner, A., Bauer, H., Kasper-Giebl,
1081   A. and Puxbaum, H.: Chemical characterisation of fine particle emissions from wood
1082   stove combustion of common woods growing in mid-European Alpine regions, Atmos.
1083   Environ., 42(1), 126–141, doi:10.1016/j.atmosenv.2007.09.028, 2008.

1084   Shi, Z., Bonneville, S., Krom, M. D., Carslaw, K. S., Jickells, T. D., Baker, A. R. and
1085   Benning, L. G.: Iron dissolution kinetics of mineral dust at low pH during simulated
1086   atmospheric processing, Atmos. Chem. Phys., 11(3), 995–1007, doi:10.5194/acp-11-
1087   995-2011, 2011.

1088   Shi, Z., Krom, M. D., Bonneville, S. and Benning, L. G.: Atmospheric processing outside
1089   clouds increases soluble iron in mineral dust, Environ. Sci. Technol., 49(3), 1472–1477,
1090   doi:10.1021/es504623x, 2015.

1091   Solmon, F., Chuang, P. Y., Meskhidze, N. and Chen, Y.: Acidic processing of mineral
1092   dust iron by anthropogenic compounds over the north Pacific Ocean, J. Geophys. Res.,
1093   114(D2), D02305, doi:10.1029/2008JD010417, 2009.

1094   Stockdale, A., Krom, M. D., Mortimer, R. J. G., Benning, L. G., Carslaw, K. S., Herbert,
1095   R. J., Shi, Z., Myriokefalitakis, S., Kanakidou, M. and Nenes, A.: Understanding the
1096   nature of atmospheric acid processing of mineral dusts in supplying bioavailable
1097   phosphorus to the oceans, Proc. Natl. Acad. Sci. U. S. A., 113(51), 14639–14644,
1098   doi:10.1073/pnas.1608136113, 2016.

1099   Straub, S. M. and Schmincke, H. U.: Evaluating the tephra input into Pacific Ocean
1100   sediments: Distribution in space and time, Int. J. Earth Sci., 87(3), 461–476, 1998.

Strzelec, M., Proemse, B. C., Gault-Ringold, M., Boyd, P. W., Perron, M. M. G., Schofield, R., Ryan, R. G., Ristovski, Z. D., Alroe, J., Humphries, R. S., Keywood, M. D., Ward, J. and Bowie, A. R.: Atmospheric trace metal deposition near the Great Barrier Reef, Australia, Atmosphere (Basel)., 11(4), 1–24, doi:10.3390/ATMOS11040390, 2020.

Tagliabue, A., Bopp, L. and Aumont, O.: Ocean biogeochemistry exhibits contrasting responses to a large scale reduction in dust deposition, Biogeosciences, 5(1), 11–24, doi:10.5194/bg-5-11-2008, 2008.

Tagliabue, A., Bopp, L., Roche, D., Bouttes, N., Dutay, J.-C., Alkama, R., Kageyama, M., Michel, E. and Paillard, D.: Quantifying the roles of ocean circulation and biogeochemistry in governing ocean carbon-13 and atmospheric carbon dioxide at the last glacial maximum, Clim. Past, 5, 695–706, 2009.

Tagliabue, A., Aumont, O. and Bopp, L.: The impact of different external sources of iron on the global carbon cycle, Geophys. Res. Lett., 41(3), 920–926, doi:10.1002/2013GL059059, 2014.

Tagliabue, A., Bowie, A. R., Boyd, P. W., Buck, K. N., Johnson, K. S. and Saito, M. A.: The integral role of iron in ocean biogeochemistry, Nature, 543(7643), 51–59, doi:10.1038/nature21058, 2017.

Textor, C., Schulz, M., Guibert, S., Kinne, S., Balkanski, Y., Bauer, S., Berntsen, T., Berglen, T., Boucher, O., Chin, M., Dentener, F., Diehl, T., Easter, R., Feichter, H., Fillmore, D., Ghan, S., Ginoux, P., Gong, S., Grini, A., Hendricks, J., Horowitz, L., Huang, P., Isaksen, I., Iversen, T., Kloster, S., Koch, D., Kirkevåg, A., Kristjansson, J. E., Krol, M., Lauer, A., Lamarque, J. F., Liu, X., Montanaro, V., Myhre, G., Penner, J., Pitari, G., Lamarque, J. F., Liu, X., Montanaro, V., Myhre, G., Penner, J., Pitari, G., Reddy, S., Seland, Ø., Stier, P., Takemura, T. and Tie, X.: Analysis and quantification of the diversities of aerosol life cycles within AeroCom, Atmos. Chem. Phys., 6, 1777–1813, doi:10.5194/acpd-5-8331-2005, 2006.

Tipping, E., Benham, S., Boyle, J. F., Crow, P., Davies, J., Fischer, U., Guyatt, H., Helliwell, R., Jackson-Blake, L., Lawlor, A. J., Monteith, D. T., Rowe, E. C. and Toberman, H.: Atmospheric deposition of phosphorus to land and freshwater, Environ. Sci. Process. Impacts, 16(7), 1608–1617, doi:10.1039/c3em00641g, 2014.

Twining, B. S. and Baines, S. B.: The trace metal composition of marine phytoplankton, Ann. Rev. Mar. Sci., 5, 191–215, doi:10.1146/annurev-marine-121211-172322, 2013.

Twining, B. S., Antipova, O., Chappell, P. D., Cohen, N. R., Jacquot, J. E., Mann, E. L., Marchetti, A., Ohnemus, D. C., Rauschenberg, S. and Tagliabue, A.: Taxonomic and nutrient controls on phytoplankton iron quotas in the ocean, Limnol. Oceanogr. Lett., doi:10.1002/lol2.10179, 2020.

Uetake, J., Hill, T. C. J., Moore, K. A., DeMott, P. J., Protat, A. and Kreidenweis, S. M.: Airborne bacteria confirm the pristine nature of the Southern Ocean boundary layer, Proc. Natl. Acad. Sci. U. S. A., 117(24), 13275–13282, doi:10.1073/pnas.2000134117, 2020.

1142 Veira, A., Kloster, S., Wilkenskjeld, S. and Remy, S.: Fire emission heights in the
1143 climate system - Part 1: Global plume height patterns simulated by ECHAM6-HAM2,
1144 Atmos. Chem. Phys., 15(13), 7155–7171, doi:10.5194/acp-15-7155-2015, 2015.

1145 Di Virgilio, G., Evans, J. P., Blake, S. A. P., Armstrong, M., Dowdy, A. J., Sharples, J.
1146 and McRae, R.: Climate Change Increases the Potential for Extreme Wildfires,
1147 Geophys. Res. Lett., 46(14), 8517–8526, doi:10.1029/2019GL083699, 2019.

1148 Wagenbrenner, N. S., Chung, S. H. and Lamb, B. K.: A large source of dust missing in
1149 Particulate Matter emission inventories? Wind erosion of post-fire landscapes, Elem Sci
1150 Anth, 5(2), 1–10, doi:10.1525/elementa.185, 2017.

1151 Wagener, T., Pulido-Villena, E. and Guieu, C.: Dust iron dissolution in seawater: Results
1152 from a one-year time-series in the Mediterranean Sea, Geophys. Res. Lett., 35(16), 1–
1153 6, doi:10.1029/2008GL034581, 2008.

1154 Wagener, T., Guieu, C. and Leblond, N.: Effects of dust deposition on iron cycle in the
1155 surface Mediterranean Sea: Results from a mesocosm seeding experiment,
1156 Biogeosciences, 7(11), 3769–3781, doi:10.5194/bg-7-3769-2010, 2010.

1157 Wagner, R., Jähn, M. and Schepanski, K.: Wildfires as a source of airborne mineral dust
1158 - Revisiting a conceptual model using large-eddy simulation (LES), Atmos. Chem.
1159 Phys., 18(16), 11863–11884, doi:10.5194/acp-18-11863-2018, 2018.

1160 Ward, D. S., Mahowald, N. M. and Kloster, S.: Potential climate forcing of land use and
1161 land cover change, Atmos. Chem. Phys., 14(8), 12701–12724, doi:10.5194/acp-14-
1162 12701-2014, 2014.

1163 Whicker, J. J., Pinder, J. E. and Breshears, D. D.: Increased Wind Erosion from Forest
1164 Wildfire: Implications for Contaminant-Related Risks, J. Environ. Qual., 35(2), 468–478,
1165 doi:10.2134/jeq2005.0112, 2006.

1166 Winton, V. H. L., Bowie, A. R., Edwards, R., Keywood, M., Townsend, A. T., van der
1167 Merwe, P. and Bollhofer, A.: Fractional iron solubility of atmospheric iron inputs to the
1168 Southern Ocean, Mar. Chem., 177, 20–32, doi:10.1016/j.marchem.2015.06.006, 2015.

1169 Winton, V. H. L., Edwards, R., Bowie, A. R., Keywood, M., Williams, A. G., Chambers,
1170 S. D., Selleck, P. W., Desservettaz, M., Mallet, M. D. and Paton-Walsh, C.: Dry season
1171 aerosol iron solubility in tropical northern Australia, Atmos. Chem. Phys., 16(19),
1172 12829–12848, doi:10.5194/acp-16-12829-2016, 2016.

1173 Wu, C., Lin, Z. and Liu, X.: Global dust cycle and uncertainty in CMIP5 models, Atmos.
1174 Chem. Phys., 5, 1–52, doi:10.5194/acp-2020-179, 2020.

1175 Yamasoe, M. A., Artaxo, P., Miguel, A. H. and Allen, A. G.: Chemical composition of
1176 aerosol particles from direct emissions of vegetation fires in the Amazon Basin: Water-
1177 soluble species and trace elements, Atmos. Environ., 34(10), 1641–1653,
1178 doi:10.1016/S1352-2310(99)00329-5, 2000.

1179 Ye, Y. and Völker, C.: On the Role of Dust-Deposited Lithogenic Particles for Iron
1180 Cycling in the Tropical and Subtropical Atlantic, Global Biogeochem. Cycles, 31(10),
1181 1543–1558, doi:10.1002/2017GB005663, 2017.

1182 Zender, C. S., Miller, R. L. and Tegen, I.: Quantifying mineral dust mass budgets :
1183 Terminology, constraints, and current estimates, Eos (Washington. DC)., 85(48),
1184 doi:10.1029/2004EO480002, 2004.

1185 Zhang, C., Ito, A., Shi, Z., Aita, M. N., Yao, X., Chu, Q., Shi, J., Gong, X. and Gao, H.:
1186 Fertilization of the Northwest Pacific Ocean by East Asia Air Pollutants, Global
1187 Biogeochem. Cycles, 33(6), 690–702, doi:10.1029/2018GB006146, 2019.

1188

SIDEBAR#1. The interface between fires and dust: in-plume dust entrainment

The impact of different agricultural-related fires on near-surface wind patterns was investigated by the idealized model study of Wagner et al. (2018), which found aerodynamic conditions suitable for dust emission in the vicinity of such fires. The simulated fire-modulated winds were coupled with two different dust emission parameterizations to obtain first estimates of the effectiveness of pyro-convectively driven dust emissions (Wagner et al., submitted to JGR). Depending on the model setup, fire-driven dust emission fluxes of 1.0-5.0 g m^{-2} h^{-1} were found, which would, if scaled up globally, account for up to 20 Tg a^{-1}. So, with respect to the total global dust emissions, estimated between 700 and 3600 Tg a^{-1} in models with comparable particle size (0.06–20 μm) (Wu et al., 2020), pyro-convectively driven dust emission could contribute an additional 3-14%, especially in regions outside the "dust-belt". Assuming a dust iron fraction of 3.5% and that 64% fire-iron is dust sourced gives emissions (<20 μm particle size) of 1.1 Tg Fe a^{-1} from fires, which is the same as a previous estimate by Luo et al. (2008).

SIDEBAR#2. The interface between fires and dust: post-burn landscape

The strength and duration of post-fire dust emissions can vary significantly depending on the geographical location, the meteorology, and the re-vegetation period. Results from

1207 several studies reflecting the geographical diversity point towards a large variability of

1208 enhanced dust fluxes between individual sites (Dukes et al., 2018; Jeanneau et al., 2019;

1209 Whicker et al., 2006). By using their averaged results as a proxy for post-burnt landscapes

1210 and assuming the periods without vegetation permitting wind erosion (months-to-year), it

1211 might be possible that such post-fire emissions can contribute in the order of magnitude

1212 of 100 Tg a^{-1} of soil dust emissions, with a possible uncertainty interval of the same order

1213 of magnitude. However, post-fire sources might at least be partly considered for global

1214 estimates on dust emission fluxes already

1215

1216 **Terms and Definitions List:**

1217 • Aerosol: solid or liquid particles suspended in the atmosphere.

1218 • Biogeochemical cycles describe how nutrients move through both the biotic and
1219 abiotic parts of the Earth System.

1220 • Major anthropogenic emissions are produced by vehicular transportation, fossil
1221 fuel and biofuel combustion, mining, intensifying agricultural practices, and metal
1222 smelting.

1223 • Macronutrients: nitrogen, phosphorus, and silicate. Micronutrients: iron, zinc,
1224 copper, cobalt, and manganese.

1225 • Net primary productivity (NPP): biomass accumulation rate from transformation
1226 of energy, in excess of respiration, by photo- or chemosynthesis.

1227 • Surface Ocean Lower Atmosphere Study (SOLAS): https://www.solas-int.org/.
1228 GEOTRACES: https://www.geotraces.org/.

1229 • Nutrient solubility: The percentage of the total aerosol that is soluble.

- Reactive nitrogen: oxidized, reduced, and organic forms of nitrogen which are bioaccessible. Examples are nitrate (NO_3^-) and ammonium (NH_4^+).

- Phosphorus: atmospheric transport occurs via aerosol as no stable gas phase exists. Phosphate (PO_4^{3-}) considered the soluble (bioaccessible) phosphorus fraction.

- Dust belt: latitudinal band including the primary dust source regions of North Africa, Arabian Peninsula, and Central Asia.

- High-Nutrient Low-Chlorophyll (HNLC) region: nitrogen and phosphorus in excess compared to biological requirements, although atypically low chlorophyll levels are observed.

- Oligotrophic: depleted in nutrients and exhibiting low surface chlorophyll. Here: Chl-a <0.5 µg L^{-1} excluding very coastal or upwelling studies.

- Coarse: Particle diameter larger than 1 or 2 µm. Fine: Particle diameter less than 1 or 2 µm.

- Smoldering: often persistent, low-temperature, flameless burning producing significant smoke volumes. Flaming: higher temperature burning with flames producing less smoke.

- Isotopic fractionation: physical, chemical, and biological processes enrich one isotope relative to another in predicable ways, creating distinct source "fingerprints".

1250   •   Pristine aerosol region: where the post-Industrial Revolution human influence on

1251   the aerosol state likely remains minimal.

1252   •   Levoglucosan: an indicator of wood combustion being derived from the pyrolysis
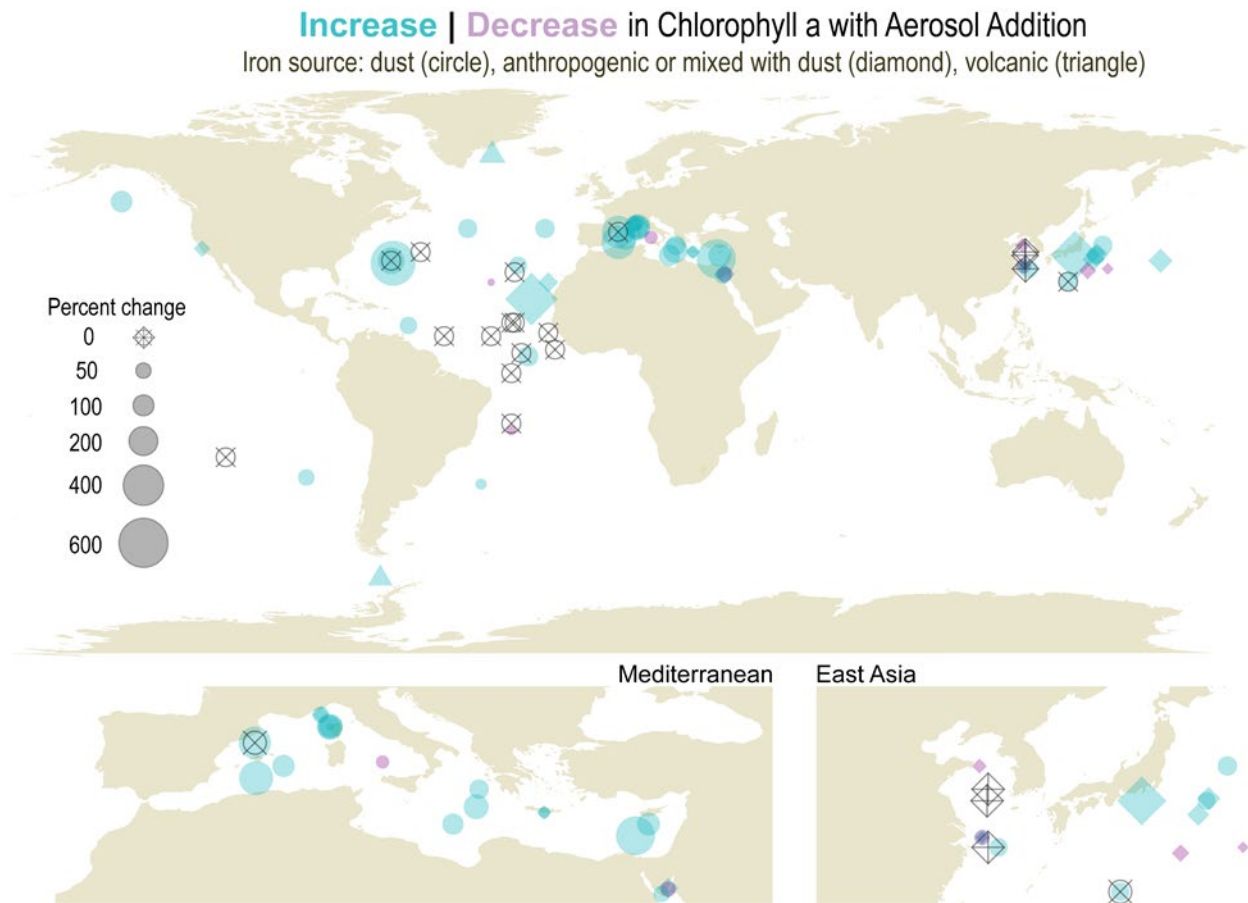
1253   of (hemi-) cellulose molecules.

1254

1255 **Figures**
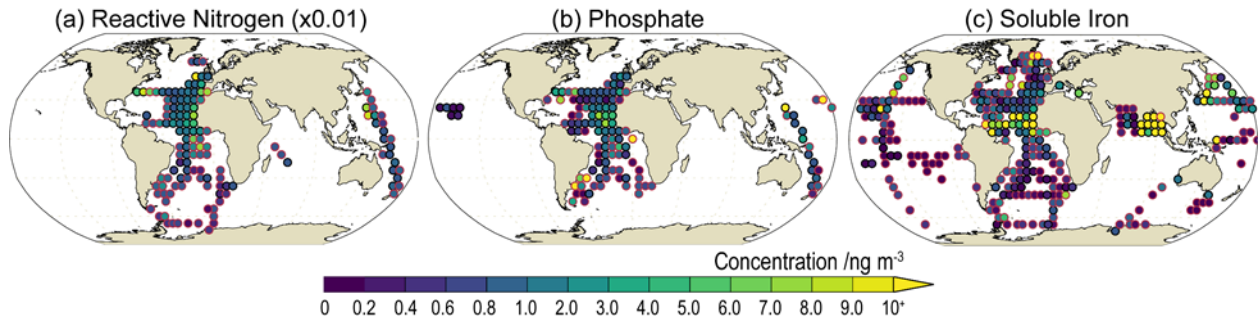
1256

1257 **Figure 1**. Ship-borne observations of atmospheric reactive nitrogen (NH_4 + NO_3 + water

1258 soluble organic nitrogen) (a), phosphate (b), and soluble iron (c) median concentrations.

1259 Observations aggregated over a 6x6 degree grid cell. Red outline indicates ≤2

1260 observations, black >2 observations.

Increase | Decrease in Chlorophyll a with Aerosol Addition
Iron source: dust (circle), anthropogenic or mixed with dust (diamond), volcanic (triangle)

Figure 2. Maximum observed biomass change, as measured by Chl-a change relative to control (bearing macro- and micronutrients and metals - including potential toxic elements such as copper) from different sources. See Table S1 for a list of the experiments, initial Chl-a values, and the citations.
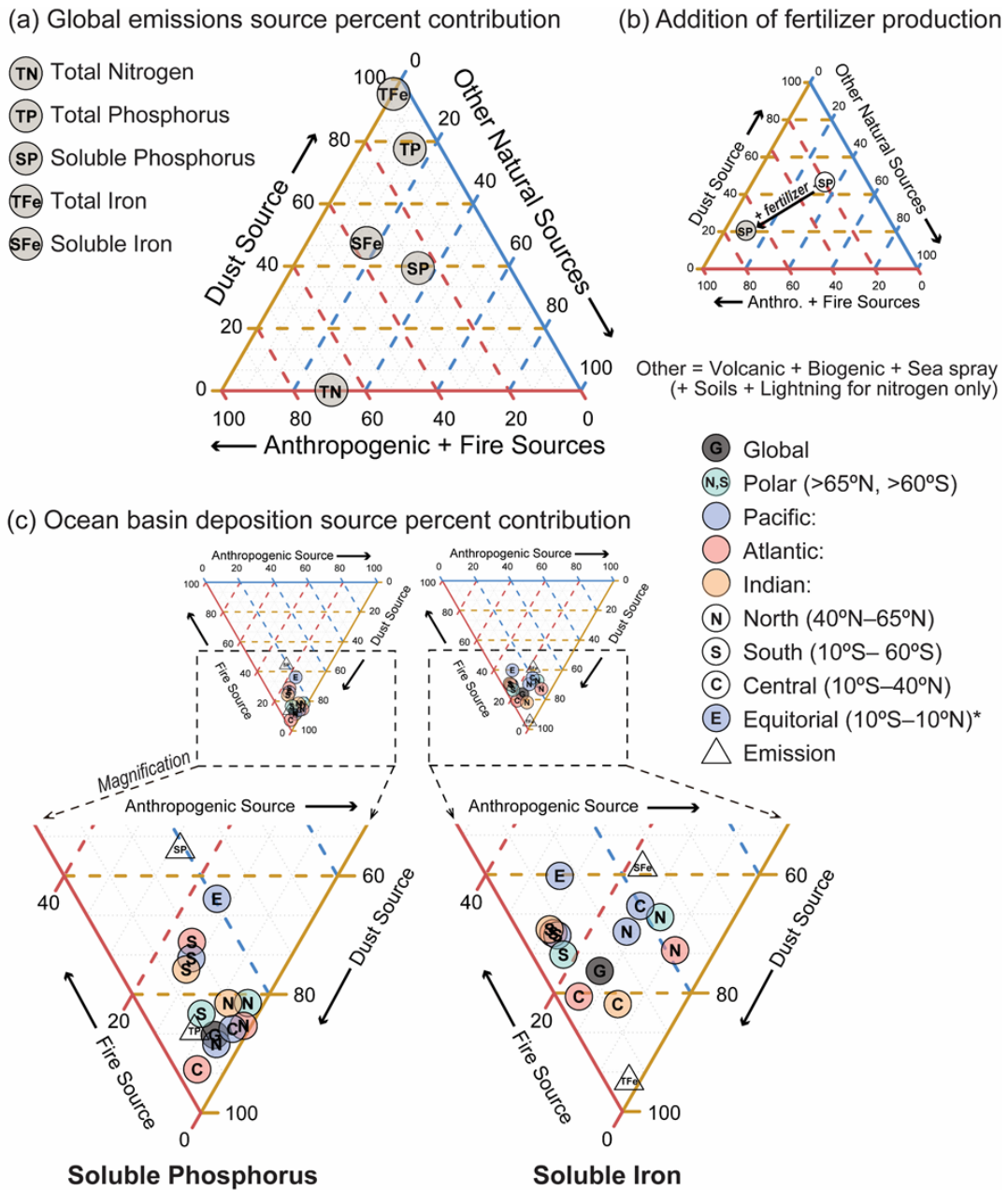
Figure 3. Percent contribution to global emissions (a), soluble phosphorus when accounting for fertilizer production (b), and ocean basin deposition (c) from each nutrient source. Emission data in (a) from Kanakidou et al., (2018) and iron modeling. Deposition data in (c) from modeling: phosphorus from Myriokefalitakis et al. (2020), iron from Table S2. (* HNLC sub-region within the central Pacific.)
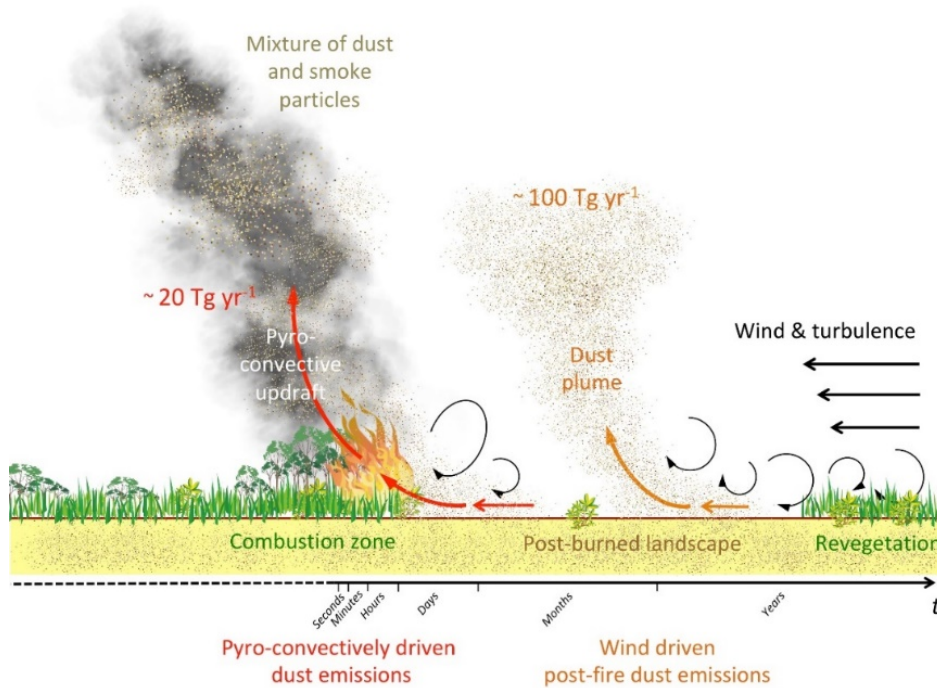
1272

Figure 4. Properties of nutrient aerosol emissions from fire activity changes with time, as well as estimates in the magnitude of aerosol fluxes. See Sidebars 1 and 2 and SI Methods for details on global annual fluxes estimated in this study.
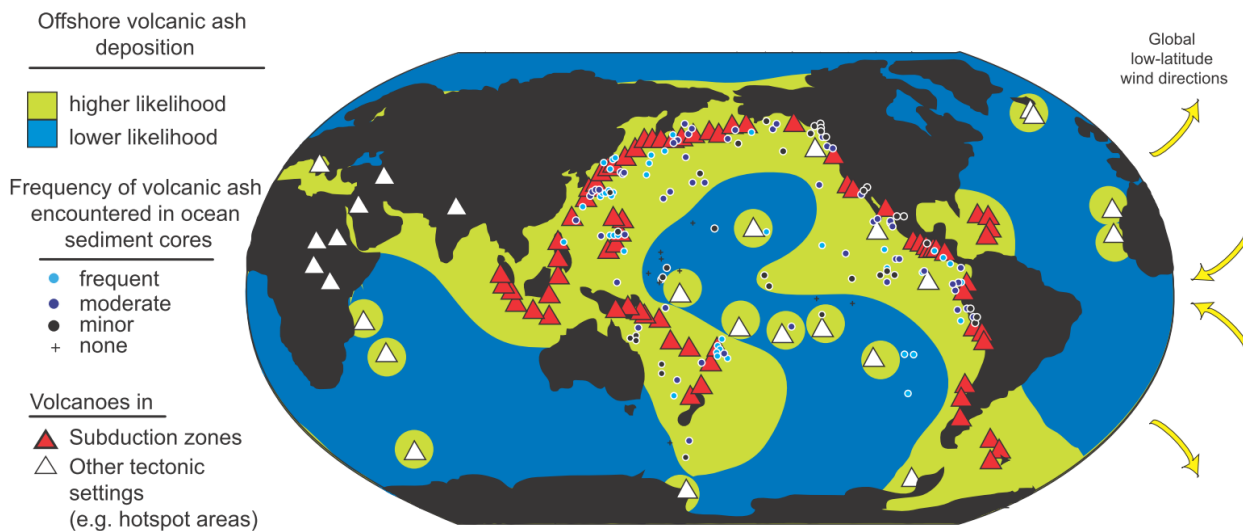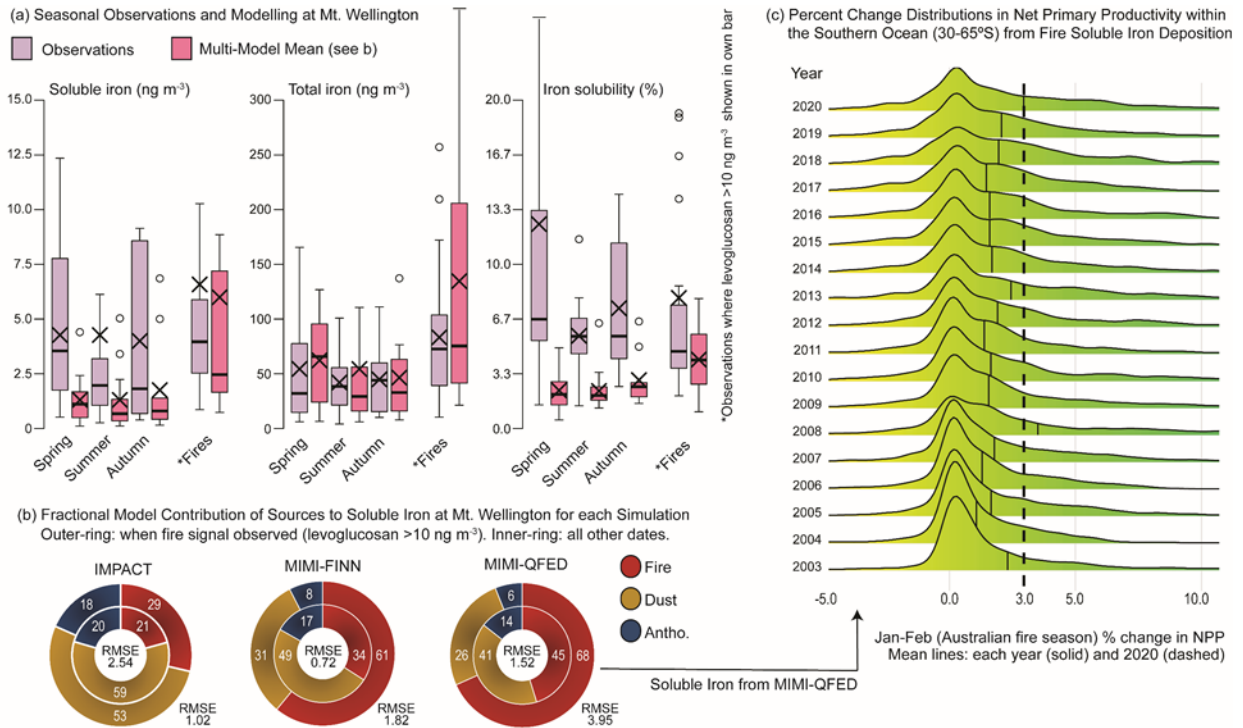

1276

Figure 5. Global distribution of volcanoes and the offshore ash deposition areas (green regions) (Olgun et al., 2011). The higher likelihood of ash deposition regions shown in

green color was based on the low-latitude wind directions and the frequency of volcanic

ash layers found in the ocean drill cores (Straub and Schmincke, 1998).

1281

Figure 6. Potential impact of wildfires on marine biogeochemistry. Observations and modeling of iron (a and b) and annual changes in January-February Southern Ocean (30–65°S) depth integrated net primary production (c). Atmospheric iron models: IMPACT (Ito et al., 2021) and MIMI (Hamilton et al., 2020b). The mean in (a) is shown by a cross (X). Levoglucosan threshold of 10 ng m^{-3} chosen to exclude residual levoglucosan levels, as previously reported in remote sampling regions (Bhattarai et al., 2019); therefore, fire observations only account for those samples displaying a distinct fire signal.

1290

Net Primary Productivity / g C a^{-1}

0   200
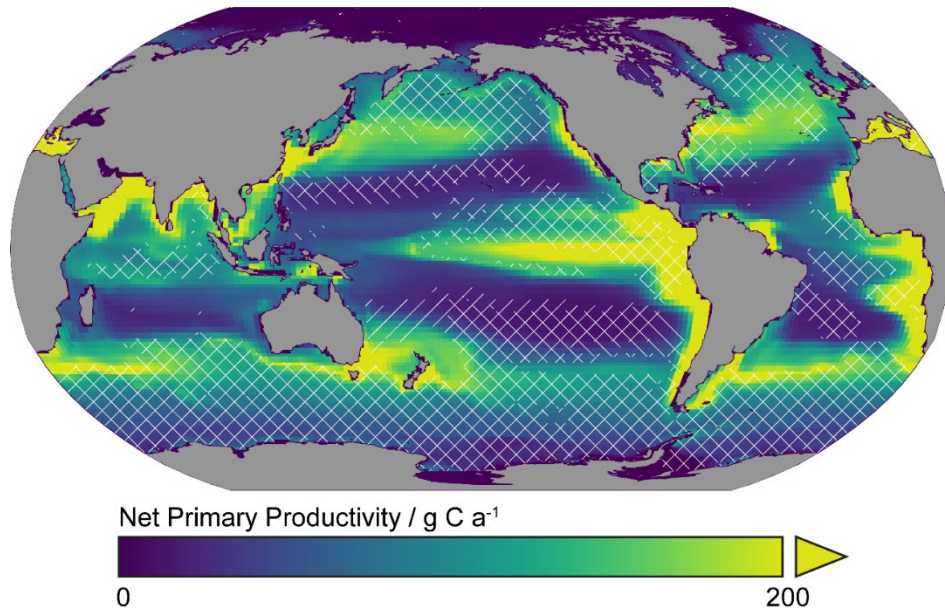
Figure 7. Annual mean (2003-2019) depth integrated marine net primary productivity. White lines indicate where fire soluble iron deposition increased productivity (different fire emission datasets are indicated by orientation: 45°=QFED, -45°=FINN; no line indicates a decrease).